Geochronology of age-progressive volcanism of the Oregon High Lava Plains: Implications for the plume interpretation of Yellowstone

Brennan T. Jordan[1] and Anita L. Grunder
Department of Geosciences, Oregon State University, Corvallis, Oregon, USA

Robert A. Duncan
College of Oceanic and Atmospheric Sciences, Oregon State University, Corvallis, Oregon, USA

Alan L. Deino
Berkeley Geochronology Center, Berkeley, California, USA

Received 2 September 2003; revised 4 June 2004; accepted 1 July 2004; published 5 October 2004.

[1] The High Lava Plains province (HLP) is a late Cenozoic bimodal volcanic field at the northern margin of the Basin and Range province in southeastern Oregon that hosts a westward younging trend of silicic volcanism that crudely mirrors northeastward migration of silicic volcanism along the Yellowstone–Snake River Plain (YSRP) trend. We present $^{40}Ar/^{39}Ar$ ages for 19 rhyolite domes, 5 rhyolite ash flow tuffs, and 34 basaltic lavas from the HLP. The previously identified trend of westward migration of HLP rhyolites is confirmed. The rate of propagation is ~33 km/m.y. from 10 to 5 Ma, slowing to ~13 km/m.y. after 5 Ma. The duration of silicic volcanism at any locus is ~2 m.y. Three older HLP dacite domes yielded ages of ~15.5 Ma. Basalts are not age progressive. We identify several episodes of increased basaltic activity at 7.5–7.8, 5.3–5.9, and 2–3 Ma, with the younger episode likely continuing into the Recent. The HLP and YSRP trends emerged from the axis of middle Miocene basaltic volcanism of the Columbia River and Steens basalts. We propose a model in which (1) Miocene flood basalts and widespread silicic rocks are the result of emplacement of a plume head near the craton margin, enhanced by flow up a topographic gradient along the base of the lithosphere at the craton margin; (2) the HLP trend is the result of westward flow originating at the craton margin; and (3) the YSRP trend is the trace of the motion of the North American plate over the tail of the plume. *INDEX TERMS:* 1035 Geochemistry: Geochronology; 8499 Volcanology: General or miscellaneous; 8121 Tectonophysics: Dynamics, convection currents and mantle plumes; 8109 Tectonophysics: Continental tectonics—extensional (0905); *KEYWORDS:* High Lava Plains, Yellowstone, argon, geochronology

Citation: Jordan, B. T., A. L. Grunder, R. A. Duncan, and A. L. Deino (2004), Geochronology of age-progressive volcanism of the Oregon High Lava Plains: Implications for the plume interpretation of Yellowstone, *J. Geophys. Res.*, *109*, B10202, doi:10.1029/2003JB002776.

1. Introduction

[2] The High Lava Plains province (HLP) of central and southeastern Oregon is a Late Tertiary to Quaternary bimodal volcanic field. Silicic volcanic rocks of the HLP are progressively younger to the west [*Walker*, 1974; *MacLeod et al.*, 1975; *McKee and Walker*, 1976; this study], generally mirroring the northeastward progression of silicic volcanic centers of the Snake River Plain to the Yellowstone Plateau [*Armstrong et al.*, 1975]. Migrating volcanism of the Yellowstone–Snake River Plain (YSRP) magmatic system is widely interpreted as the trace of a mantle plume now under Yellowstone [e.g., *Pierce and Morgan*, 1992; *Smith and Braille*, 1994]. The existence of the antithetic HLP trend is often cited as evidence against this hypothesis [e.g., *Christiansen and McKee*, 1978; *Hamilton*, 1989; *Christiansen et al.*, 2002]. Proponents of the plume interpretation note differences between the trends and suggest that they are not linked [*Pierce and Morgan*, 1992], or that the HLP trend may not be a robust feature [*Smith and Braille*, 1994].

[3] The HLP separates the Basin and Range extensional province from the less extended Blue Mountain province

[1]Now at Department of Geology, College of Wooster, Wooster, Ohio, USA.

0148-0227/04/2003JB002776$09.00

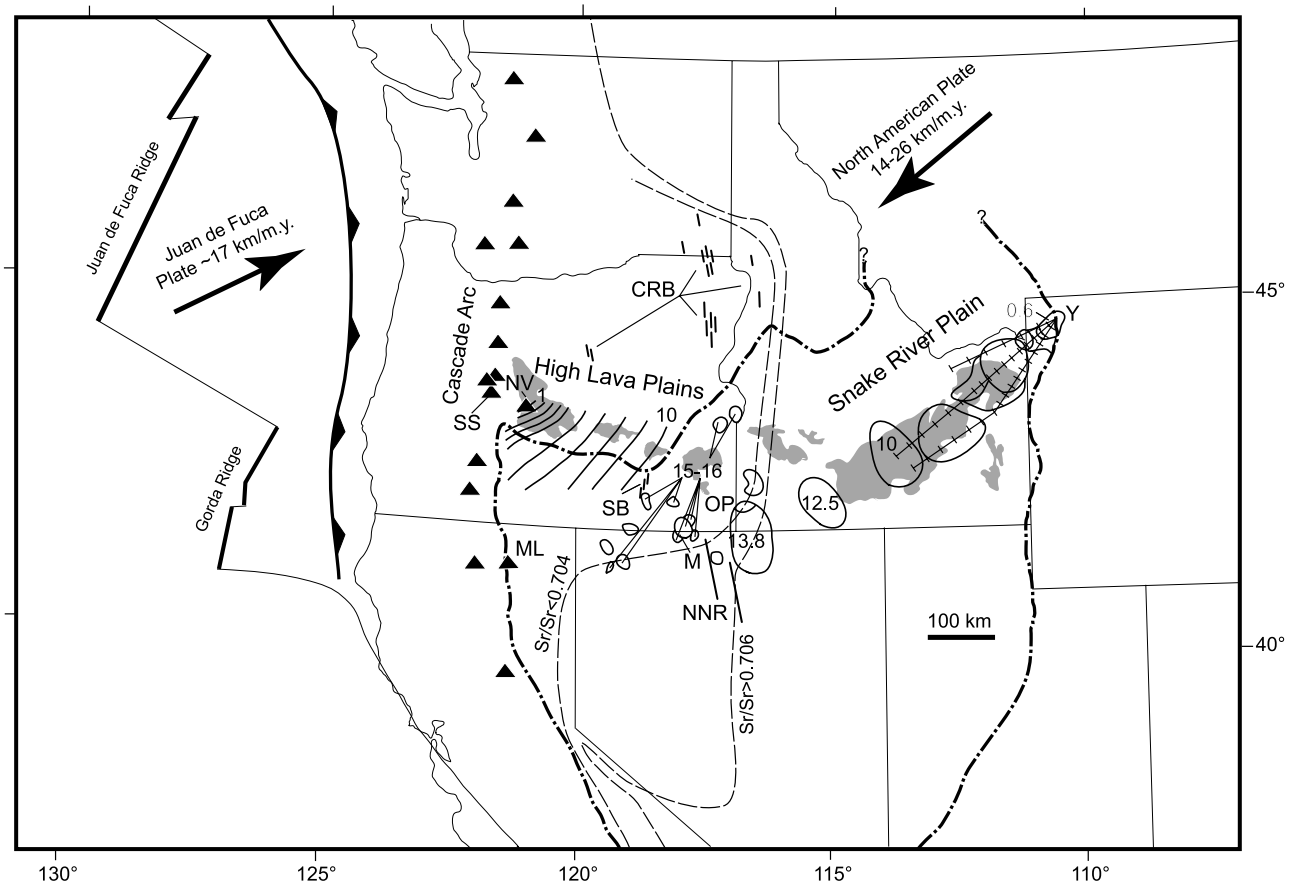

Figure 1. Map showing the tectonic setting of the Oregon High Lava Plains (HLP) and Snake River Plain. Y, Yellowstone; M, McDermitt volcanic field; OP, Owyhee Plateau; NV, Newberry volcano; SS, South Sister; ML, Medicine Lake volcano. Pliocene and younger basalts of the HLP and YSRP are shaded. The bold dash-dotted line shows the limit of Basin and Range extension. Curved lines cutting across the HLP and northwestern Basin and Range are isochrons of silicic volcanism (from Figure 3); 10 Ma and 1 Ma are labeled. Circled areas are volcanic centers of the Yellowstone-Snake River Plain (YSRP) and Owyhee region [after *Pierce and Morgan*, 1992]; ages are given for some calderas to indicate age progression, with many volcanic centers identified in the range 15–16 Ma. Also shown are dike complexes that fed middle Miocene flood basalts; CRB, Columbia River basalt dikes; SB, Steens Basalt dikes; NNR, Northern Nevada Rift. Ticked lines (ticks represent 1 m.y. intervals) across the YSRP are back-projected from Yellowstone to show the lengths of hot spot tracks predicted by global plate motion models plus extension (the northern line is based on the model of *Gripp and Gordon* [2002] which extends only to 6 Ma, the period of the model; line middle is based on the model of *Müller et al.* [1993], and the southern line is based on the model of *Duncan and Richards* [1991]). The light dashed lines indicate approximate positions of the Sr isotope discontinuities (after synthesis of *Ernst* [1988]); the 0.706 line is thought to broadly delineate the craton margin.

to the north; to the west, the HLP impinges upon the Cascade Range (Figure 1). Previous models relate the HLP trend to processes active in the adjacent provinces. *Christiansen and McKee* [1978] and *Christiansen et al.* [2002] propose that the HLP trend is the result of a propagating shear zone accommodating the northward termination of Basin and Range extension. *Carlson and Hart* [1987] relate middle Miocene magmatism and subsequent propagation of HLP silicic volcanism to a back arc setting, and a change in the geometry of subduction. *Draper* [1991] proposes that the HLP trend reflects the entrainment of plume head material in subduction-induced, asthenospheric counter flow. *Humphreys et al.* [2000] refine this model, proposing that both the HLP and YSRP trends could result from mantle flow around the buoyant residuum of middle Miocene magmatism (of uncertain origin) in the shear fields created by plate motion and subduction counterflow.

[4] The problem of complex patterns of migrating volcanism posed by the HLP and YSRP trends has been recognized as one of the outstanding puzzles in understanding volcanism in the Pacific Northwest [*Swanson*, 1982]. We present new $^{40}Ar/^{39}Ar$ single-crystal total fusion and bulk incremental heating ages for rhyolites and basalts of the

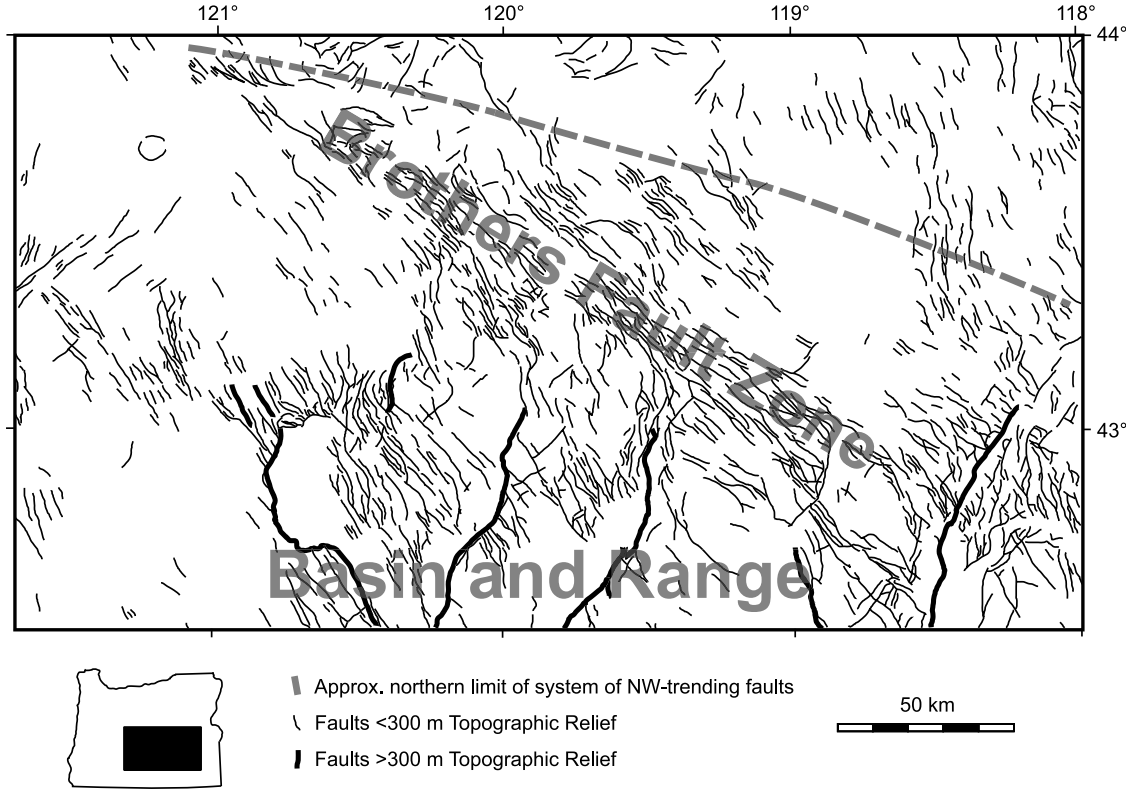

Figure 2. Map of faults of the High Lava Plains and northwestern Basin and Range [after *Walker and MacLeod*, 1991].

HLP and consider the bearing of these ages on the origin of the HLP trend and the potential relationship between the HLP and YSRP trends.

2. The High Lava Plains

2.1. Volcanic Rocks

[5] The HLP is underlain by widespread, thin lava flows of basalt intercalated with rhyolitic ash flow tuffs and tuffaceous sediments and punctuated by rhyolite dome complexes. It is strongly a bimodal volcanic province with only 8% of a compilation of 286 analyzed samples being andesites or dacites; this value probably overrepresents intermediate compositions because of preferential sampling of these petrologically important units.

[6] Basalts are mostly tholeiites (the high-alumina olivine tholeiites of *Hart et al.* [1984]), though basaltic andesites, some of which are calc-alkaline, constitute approximately a quarter of analyzed mafic samples. HLP basalts are generally aphanitic to sparsely porphyritic with common plagioclase (up to 1 cm) and olivine (up to 3 mm), the typical phenocryst assemblage. Clinopyroxene phenocrysts are present in some unusually incompatible-element-enriched basalts and basaltic andesites. Glomerophyric clusters, including two or three phenocryst phases are common in evolved basalts and basaltic andesites. Most basalts have a diktytaxitic texture, although other groundmass textures include intergranular, subophitic, and ophitic.

[7] Rhyolites erupted in more than 60 domes and dome complexes, three major ash flow sheets (Prater Creek Tuff, Devine Canyon Tuff, and Rattlesnake Tuff), and several minor tuffs. Silicic rocks are mainly high-silica rhyolites (>75 wt% SiO_2) and are metaluminous to mildly peralkaline. Rhyolite lavas and tuffs are aphanitic to moderately porphyritic, with varying combinations of plagioclase, quartz, sanidine or anorthoclase, biotite, hornblende, and clinopyroxene phenocrysts [*MacLean*, 1994; *Streck and Grunder*, 1995; *Johnson and Grunder*, 2000]. Intermediate composition volcanic rocks are uncommon among rocks younger than 11 Ma and mainly result from mixing of mafic and silicic compositions [*Linneman and Meyers*, 1990; *MacLean*, 1994; *Streck and Grunder*, 1999].

2.2. Structure

[8] The transition from the Basin and Range province to the High Lava Plains is manifested by a northward decrease in relief on fault-bounded range fronts and a diffuse zone of northwest striking normal faults (Figure 2). The system of northwest trending faults occurs in the HLP and 150 km south into the Basin and Range. An apparent concentration of these faults that cuts obliquely the HLP was termed the Brothers Fault Zone by *Walker* [1969]. *Lawrence* [1976] identified several other apparent concentrations of these faults to the south (the Eugene-Denio and McLaughlin zones) and the east (the Vale zone). We note that northwesterly faults pervade the northern Basin and Range and that much of what separates these fault zones is cover by basin fill. We consider these fault zones to constitute one diffuse system.

[9] In the HLP the northwest trending faults are closely spaced (1–2 km) and generally several km long, with en echelon overlap at fault tips. The offset on these faults is

generally a few tens of meters, to occasionally over 100 m. Because of limited erosion across fault scarps, exposed fault planes and kinematic indicators are rare. Where exposed, fault planes dip steeply (70–80°) and the offset is normal. Both Basin and Range and Brothers Fault Zone faults were active in the eastern HLP by ~10 Ma [*Johnson and Grunder*, 2000].

2.3. Previous Geochronology

[10] The westward migrating pattern of silicic volcanism of the HLP and northwestern Basin and Range was first recognized by the regional reconnaissance mapping and K-Ar geochronology of *Walker* [1974] and *McKee and Walker* [1976] and was illustrated as a series of isochrons by *MacLeod et al.* [1975] (see Figure 3). No age progression was observed for basalts of the HLP [cf. *Draper*, 1991]. In a statewide compilation of K-Ar age determinations, *Fiebelkorn et al.* [1983] reported other scattered published and unpublished ages for rhyolites and basalts and corrected previously reported ages for the currently accepted ^{40}K decay constant [*Steiger and Jäger*, 1977]. Ages determined for rhyolites and basalts of the HLP and northwestern Basin and Range since the *Fiebelkorn et al.* [1983] are compiled in Figures 3 and 4.

3. Methods

[11] Samples were analyzed by the ^{40}Ar/^{39}Ar technique in two laboratories. A suite of 23 samples consisting primarily of rhyolites was analyzed at the Berkeley Geochronology Center, and 36 samples, primarily basalts, were analyzed in the College of Oceanic and Atmospheric Sciences at Oregon State University.

3.1. Berkeley Geochronology Center

[12] Samples analyzed at the Berkeley Geochronology Center included 18 rhyolite and dacite lavas, four rhyolitic tuffs, and one basalt. Lavas and tuffs were prepared as sanidine, biotite, and plagioclase mineral separates or crushed obsidian except for one tuff which was prepared as a separate of devitrified matrix material (Tables 1 and 2). The basalt was prepared as crushed whole rock. Samples numbered HP-91-X were irradiated in the central thimble facility of the Omega West reactor of the Los Alamos National Laboratory without the use of Cd shielding. All other samples were irradiated in the Cd-shielded cadmium-lined, in-core irradiation tube (CLICIT) facility of the Oregon State University (OSU) TRIGA reactor. Samples were regularly interspersed with monitor standards in wells drilled in a concentric circular pattern on aluminum disks. Sanidine from the Fish Canyon Tuff, with reference age 28.02 Ma [*Renne et al.*, 1994] was used as the neutron fluence monitor.

[13] Seventeen samples were analyzed by the laser total fusion method using a focused Ar ion or Nd-YAG laser (Table 1). In these experiments, 6 to 15 single grains of sanidine, plagioclase, or obsidian glass were analyzed per sample. Four samples were analyzed by incremental heating using a defocused Ar ion laser, all of which were run in duplicate (Table 2). Samples for laser fusion or heating were loaded into a copper sample holder and baked at 200°C overnight. Two samples were heated incrementally employing a double-vacuum resistance furnace (Table 2). Isotopic measurements were made in a Mass Analyzer Products MAP-215/50 noble gas mass spectrometer.

3.2. Oregon State University

[14] Samples analyzed at OSU (Table 3) were prepared as either whole rock minicores (~100 mg), groundmass separates, or mineral separates (plagioclase). Samples and monitors (Fish Canyon Tuff biotite, FCT-3, with a reference age of 28.02 Ma [*Renne et al.*, 1994]) were stacked in quartz tubes and irradiated at the TRIGA reactor facility at OSU. Samples were degassed at 400°C for 20 min then analyzed in a series of stepwise heating experiments with increments ranging from 50 to 200°C to optimize instrumental operating parameters. Samples were heated in a low-blank tantalum resistance furnace with a programmable electronic control unit. Gases produced during heating were cleaned by sequential exposure to Zr-Al getters. Analyses were made with a Mass Analyzer Products MAP-215/50 mass spectrometer operating in peak-hopping mode [*Duncan and Hogan*, 1994; *Duncan et al.*, 1997].

4. Results

[15] Of the 201 laser total fusion analyses summarized in Table 1, six fell more than two standard deviations beyond their weighted mean sample ages and were rejected from further analysis. Age probability spectra for the remaining laser total fusion ages are near Gaussian for 18 samples, while one sample (HP-91-2) yielded a bimodal distribution (Figures 5 and 6). Good correspondence in mean age was found between coexisting sanidine and nonhydrated obsidian (HP-91-10), and between sanidine and plagioclase (HP-91-14).

[16] In all but one of the incremental heating experiments conducted at the Berkeley Geochronology Center (Table 2), incremental heating spectra yielded apparent age plateaus using the definition of *Fleck et al.* [1977] (three or more

Figure 3. Map of the High Lava Plains showing the distribution of rhyolites. The locations of ^{40}Ar/^{39}Ar ages presented in this paper are shown (solid squares, as reported in Tables 1–3), as well as previous age determinations (open squares, reported to one digit past decimal), where not superceded by new ages. The gray dashed line is from Figure 2 and indicates the northern extent of the system of closely spaced northwest trending faults. The striped lines are isochrons (in 1 m.y. increments) marking the arrival of silicic volcanism in an area. In recognition of the 2 m.y. duration of volcanism at any given point, the isochrons are not drawn to fit every point, but rather such that there are no older ages on the younger side of an isochron and all ages are within 2 m.y. of the interpolated isochron. Previous ages are from the summaries of *Fiebelkorn et al.* [1983], *Hart et al.* [1984], *Diggles et al.* [1990], *Pickthorn and Sherrod* [1990], and *Johnson* [1998]. The 15.9 Ma age is the weighted mean of two ages reported by *Fiebelkorn et al.* [1983] for a rhyolite dome near Venator. The Harney Basin (HB) and Newberry caldera (NC) are shown.

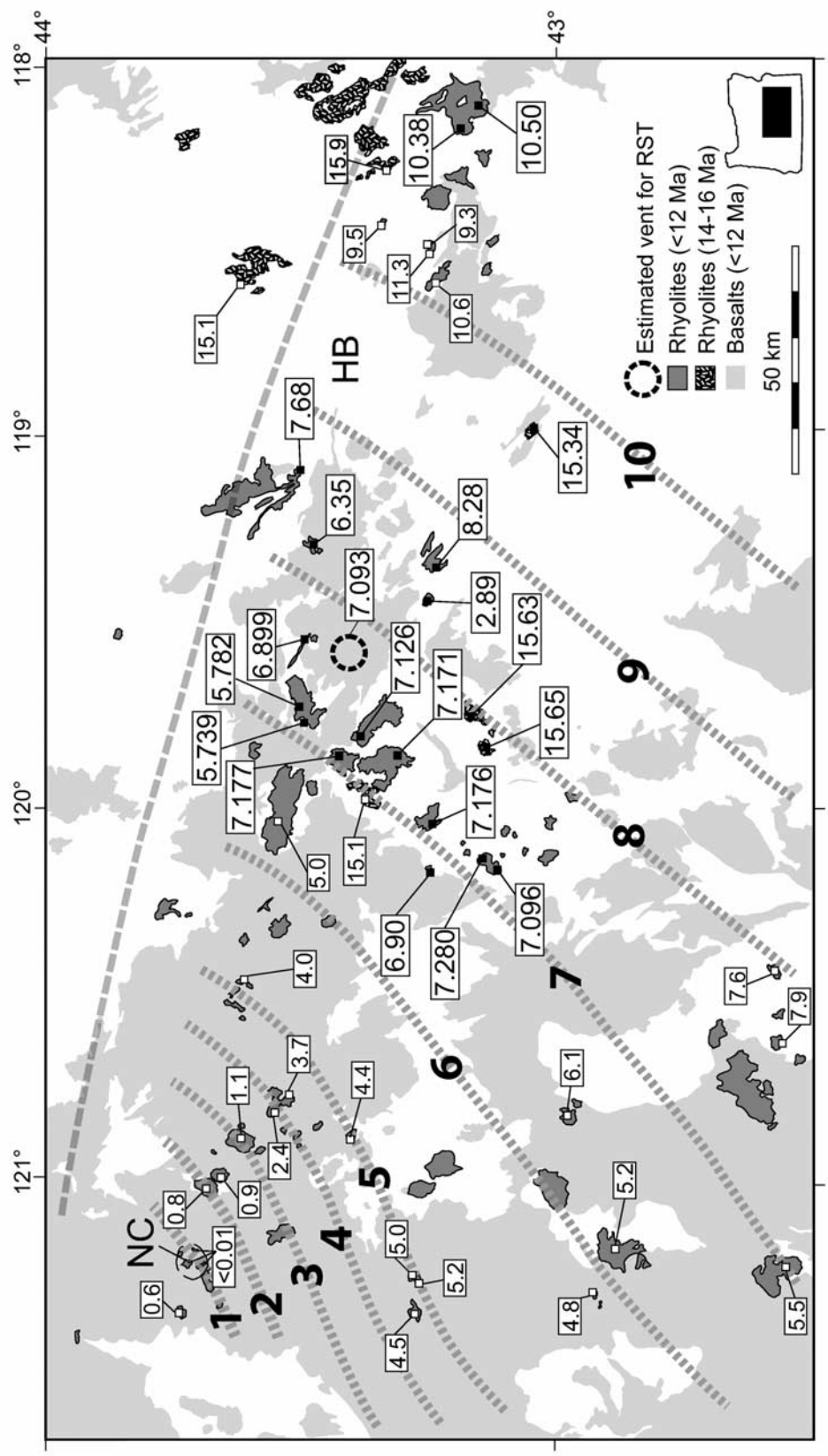
118°
119°
120°
121°
44°
43°
HB
NC
1
2
3
4
5
6
7
8
9
10
Estimated vent for RST
Rhyolites (<12 Ma)
Rhyolites (14-16 Ma)
Basalts (<12 Ma)
50 km
15.9
10.38
10.50
9.5
9.3
11.3
10.6
15.1
7.68
15.34
6.35
8.28
7.093
2.89
6.899
15.63
5.782
7.126
7.171
5.739
15.65
7.177
7.176
5.0
15.1
6.90
7.280
7.096
4.0
7.6
7.9
3.7
1.1
4.4
6.1
2.4
0.9
0.8
5.2
<0.01
5.0
0.6
5.2
4.8
5.5
4.5

Figure 3

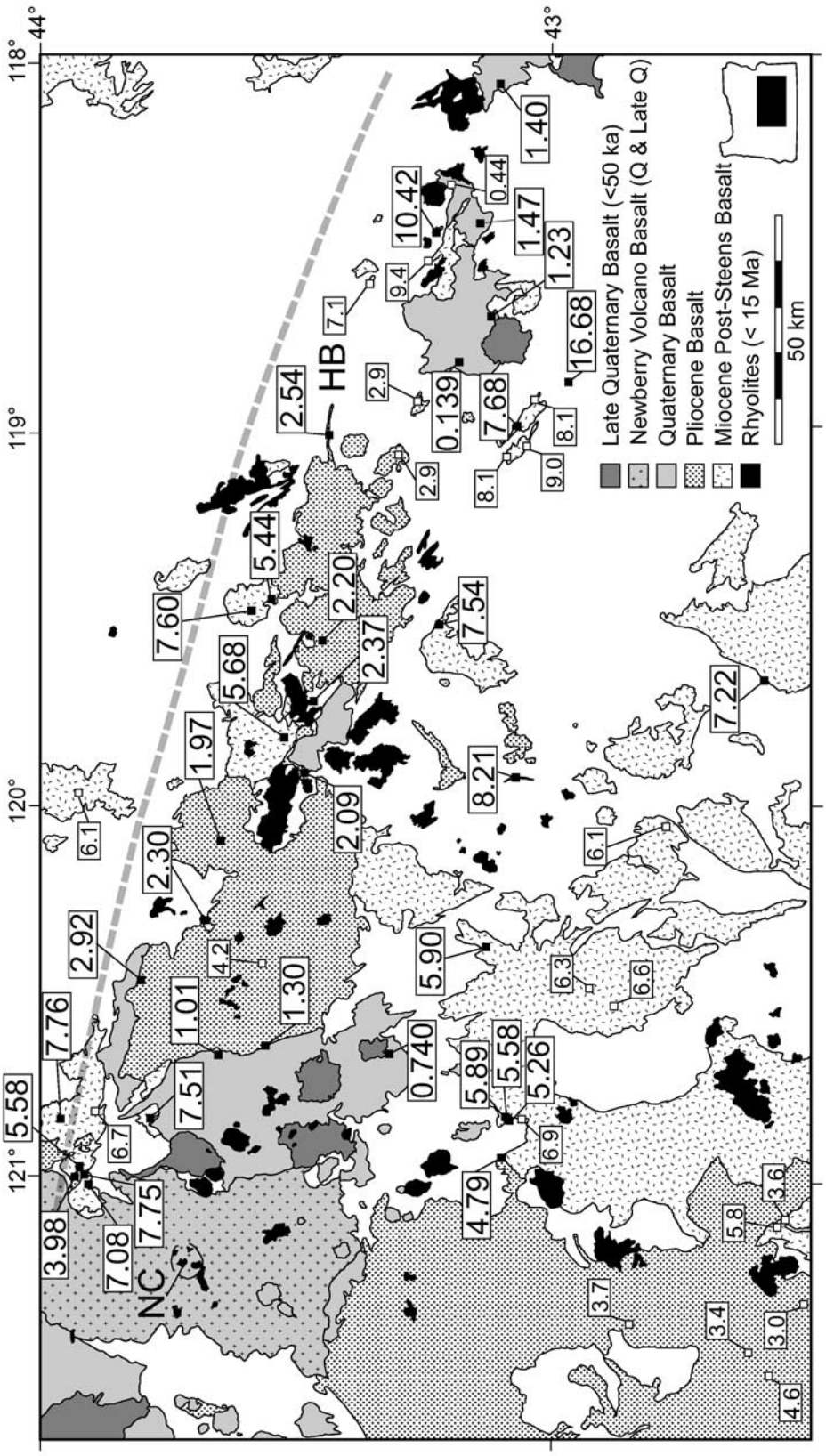

Figure 4. Map of the High Lava Plains showing the distribution of basalts. See Figure 3 caption for full description.

Table 1. Laser Total Fusion Age Determinations, Berkeley Geochronology Center[a]

Sample	Dome or Tuff	Rock Type[b]	Material Dated[c]	Number of Analyses Accept/Total	Average Percent Radiogenic ^{40}Ar	Weighted Mean Age, Ma	±1σ
DC-215a	Devine Canyon Tuff	AFT	S	9/10	98.7	**9.74**	**0.02**
DO-93-13	Double-O Ranch	R	P	13/14	81.0	**8.28**	**0.05**
HP-91-2	Burns Butte	R	S	8/9	66.8	**7.68**[d]	**0.04**
HP-91-7	Little Juniper Mountain	D	S	8/8	93.5	**15.65**	**0.04**
HP-91-9	Buckaroo Lake Tuff	AFT	S	10/10	87.4	**6.85**	**0.04**
HP-91-10	Horse Mountain	D	O	9/9	96.3	7.095	0.018
			S	10/10	89.1	7.096	0.030
						7.096[e]	**0.015**[e]
HP-91-12	Rattlesnake Tuff	AFT	S	15/15	95.7	**7.093**	**0.015**
HP-91-13	Juniper Ridge, west	R	S	15/15	89.8	**5.739**	**0.016**
HP-91-14	Horsehead Mountain	D	P	9/9	85.9	15.57	0.10
			S	6/6	98.0	15.64	0.03
						15.63[e]	**0.03**[e]
HP-93-2	Sheep Mountain	R	S	12/12	97.1	**7.177**	**0.014**
HP-93-4	Egli Ridge, northwest	R	O	9/10	97.8	**7.126**	**0.015**
HP-93-13C	Wagontire Mountain	R	O	7/8	80.6	**7.171**	**0.018**
HP-93-16	Horse Mountain, north	R	S	14/15	92.0	**7.280**	**0.016**
HP-93-25	Ram's Butte	R	S	12/12	93.7	**7.176**	**0.014**
JJ92-5	Indian Creek Butte	RD	S	10/10	98.5	**10.38**	**0.03**
JR-91-25	Juniper Ridge, west	R	O	10/10	86.7	**5.782**	**0.018**
JR-92-56	Juniper Ridge, east	R	O	10/10	98.1	**6.899**	**0.019**

[a]Bold typeface, preferred age.
[b]AFT, ash flow tuff; R, rhyolite; RD, rhyodacite.
[c]S, sanidine; P, plagioclase; O, obsidian.
[d]Age of HP-91-2 which is uncertain due to bimodal nature of probability-age spectrum.
[e]Weighted mean of two determinations.

contiguous steps concordant at 2σ, and constituting greater than 50% of the ^{39}Ar released in the incremental heating experiment). Data were also plotted on $^{36}Ar/^{40}Ar$-$^{39}Ar/^{40}Ar$ isochron diagrams (''inverse isochron''). Plateau ages are concordant with the isochron ages calculated from plateau steps, with isochrons meeting the statistical population criteria of mean sum of weighted deviates less than critical values defined by *Mahon* [1996]. In accordance with standard procedures at the Berkeley Geochronology Center we accept the isochron age as the preferred age. For samples which were run in duplicate, by either incremental heating or laser total fusion, the weighted mean of both ages is reported and taken to be the best estimate of the age of the sample. Some of the ages determined at the Berkeley Geochronology Center have been previously reported [e.g., *Streck and Grunder*, 1995; *Johnson and Grunder*, 2000; *Jordan et al.*, 2002a] but are here revised with reference to the most current age of the Fish Canyon Tuff standard [*Renne et al.*, 1994].

[17] Of the 39 incremental heating experiments conducted at Oregon State University (Table 3), 28 yielded

Table 2. Incremental Heating Age Determinations, Berkeley Geochronology Center[a]

					Plateau			Isochron			Integrated		
Sample	Dome or Tuff	Rock Type[b]	Material Dated[c]	Heating Device[d]	Age, Ma	±1σ	^{39}Ar, %	Age, Ma	±1σ	$^{40}Ar/^{36}Ar$ Intercept	±1σ	Age, Ma	±1σ
HP-91-4	Palomino Butte	R	Bt	L	6.33	0.03	71	**6.35**	**0.03**	284	4	6.25	0.06
			Bt	L	-	-	-	-	-	-	-	6.29	0.08
HP-91-5	Iron Mountain	R	Bt	L	2.85	0.04	58	2.79	0.12	310	25	2.63	0.11
			Bt	L	2.80	0.11	92	2.98	0.11	283	6	2.62	0.30
								2.89[e]	**0.08**[e]				
HP-91-11	Elk Butte	R	Bt	L	6.92	0.03	84	6.90	0.03	298	3	6.71	0.07
			Bt	L	6.92	0.04	82	6.90	0.04	297	2	6.54	0.10
								6.90[e]	**0.02**[e]				
JJ92-1	Duck Creek Butte	R	Bt	L	10.48	0.04	98	10.50	0.04	290	6	10.41	0.07
			Bt	L	10.50	0.03	100	10.52	0.06	289	12	10.49	0.10
								10.50[e]	**0.03**[e]				
JJ92-20	Lava near Duck Creek Butte	B	WR	F	1.38	0.04	92	1.42	0.05	294	2	1.25	0.16
			WR	F	1.30	0.06	100	1.38	0.06	292	2	1.21	0.20
								1.40[e]	**0.04**[e]				
PC-1	Prater Creek Tuff	AFT	matrix	F	8.46	0.09	70	**8.41**	**0.16**	350	160	8.46	0.09

[a]Bold typeface, preferred age.
[b]AFT, ash-flow tuff; R, rhyolite; B, basalt.
[c]Bt, biotite; WR, whole rock.
[d]L, laser; F, furnace.
[e]Weighted mean of two determinations.

Table 3. Incremental Heating Age Determinations, Oregon State University[a]

			Plateau					Isochron					Integrated	
Sample	Rock Type[b]	Material Dated[c]	Age (Ma)	±(1σ)	Steps Plateau	^{39}Ar, %	Plateau MSWD	Age, Ma	±1σ	^{40}Ar/^{36}Ar Intercept	±1σ	Isochron MSWD	Age, Ma	±1σ
1WHLP99	B	WR	**7.08**	**0.13**	5	100	1.31	7.05	0.26	301.0	20.7	1.49	6.95	0.22
2WHLP97	B	WR	7.90	0.13	-	83	-	**7.75**	**0.12**	307.4	4.4	1.95	8.04	0.14
6WHLP98	B	WR	**5.58**	**0.06**		100		5.56	0.09	296.6	5.1		5.60	0.07
8WHLP97	B	WR	**3.98**	**0.06**	3	60	2.02	3.93	0.06	305.8	5.3	0.00	4.06	0.06
13WHLP98	B	WR	**5.58**	**0.11**	6	96	1.17	5.46	0.14	316.2	16.6	1.01	6.07	0.13
15WHLP98	B	WR	**5.26**	**0.09**	8	100	0.37	5.28	0.13	293.9	10.1	0.41	5.17	0.17
24WHLP98	B	WR	**5.89**	**0.12**	4	74	2.36	5.76[d]	0.31	305.0	22.2	3.23	6.73	0.13
25WHLP98	B	GM	**0.740**	**0.059**	8	100	0.70	0.467	0.177	302.7	6.7	0.58	0.806	0.072
		WR	-	-	-	-	-	-	-	-	-	-	1.84	0.12
30WHLP98	B	WR	-	-	-	-	-	-	-	-	-	-	1.59	0.13
48WHLP98	B	WR	7.95	0.08	4	66	1.19	**7.51**[e]	**0.08**	317.3	4.6	0.46	8.06	0.33
74WHLP98	B	WR	**7.76**	**0.13**	6	92	2.40	7.76[d]	0.12	296.0	6.5	2.18	7.61	0.13
76WHLP98	B	Pl	-	-	-	-	-	-	-	-	-	-	234	25
		WR	**1.01**	**0.07**		66		0.68	0.25	311.6	20.0		1.48	0.06
81WHLP98	B	WR	1.74	0.16	6	98	0.30	**1.30**	**0.17**	301.6	1.8	0.19	1.82	0.14
103WHLP98	B	WR	**4.79**	**0.11**	7	100	0.90	4.63	0.23	396.6	117.4	1.00	4.89	0.28
123WHLP98	B	WR	**2.30**	**0.15**	-	78	-	2.08	0.38	311.7	30.0	1.40	2.70	0.15
128WHLP98	B	GM	**2.92**	**0.06**	7	99	0.96	2.82	0.09	307.7	7.9	0.53	2.77	0.11
130WHLP98	B	WRR	**1.97**	**0.21**	4	74	1.01	1.82	0.39	303.5	13.7	1.09	1.45	0.33
138CHLP98	B	GM	-	-	-	-	-	-	-	-	-	-	14.25	2.97
143CHLP98	B	WRR	8.00	0.33		69		**5.68**[e]	**0.40**	308.5	1.6		10.11	0.38
145CHLP98	B	WRR	**2.20**[f]	**0.04**	2	56	*0.95*	-	-	-	-	-	2.36	0.05
148CHLP98	B	WRR	-	-	-	-	-	**7.54**	**0.13**	322.0	1.8	0.53	10.12	0.13
HBA-13.5	B	WRR	**7.60**	**0.11**	3	62	0.69	7.87	0.24	288.6	5.7	0.00	6.37	0.26
HBA-3	B	WRR	**5.44**	**0.10**	9	52	1.99	5.02	0.27	320.6	15.1	0.62	5.59	0.14
HLP-98-6a	AFT	P	12.03	0.51	14	100	1.04	**8.45**	**0.96**	304.1	2.2	0.48	13.83	0.63
HLP-98-12	B	WRR	**5.90**	**0.09**	5	94	0.83	5.16	0.63	317.5	18.8	0.47	5.60	0.19
HLP-98-24	B	WRR	**7.21**	**0.22**	7	100	0.95	6.92	0.29	315.1	11.5	0.34	6.54	0.51
HLP-98-32	D	P	**15.34**	**0.19**	8	100	0.91	14.79	0.54	310.4	13.5	0.70	14.85	0.69
HLP-98-33	B	WR	**7.68**	**0.08**	5	68	1.12	7.54	0.11	313.8	10.9	0.45	8.03	0.07
HLP-98-35	B	WR	**16.68**	**0.13**	3	73	0.51	16.49	0.24	301.5	6.3	0.12	16.62	0.23
HLP-98-40	B	WR	**1.23**	**0.05**	5	91	0.79	1.21	0.06	304.0	11.0	0.76	1.02	0.13
HLP-98-42	B	WR	**1.47**	**0.08**	4	91	0.40	1.39	0.37	298.1	10.9	0.55	1.34	0.17
HLP-98-54	B	GM	**10.42**	**0.06**	7	89	1.81	10.37	0.09	300.1	4.0	1.75	10.64	0.11
HLP-98-59	B	WR	**0.139**	**0.081**	3	81	0.05	0.162	0.261	291.5	39.3	0.10	0.542	0.164
HLP-98-66	B	WR	**2.54**	**0.07**	7	93	0.58	2.50	0.09	321.8	27.8	0.49	2.72	0.09
HP-93-29	B	WR	**2.09**	**0.18**		78		1.13	0.33	302.6[g]	2.6		2.97	0.17
HP-33	B	WR	**8.21**	**0.43**	9	100	0.43	7.64	0.61	303.8	6.2	0.22	8.23	0.46
JR-91-21	B	WR	**2.37**	**0.04**	7	89	0.49	2.42	0.07	269.2	33.1	0.41	2.36	0.07

[a]Bold typeface, preferred age.
[b]B, basalt; AFT, ash-flow tuff; D, dacite.
[c]WR, whole rock; GM, groundmass; P, plagioclase.
[d]Isochron MSWD exceeding critical value.
[e]Plateau based on selected steps, isochron based on all steps.
[f]Two-step plateau.
[g]The ^{40}Ar/^{36}Ar intercept beyond atmospheric ratio, but poorly constrained by low ^{39}Ar/^{40}Ar.

plateaus with ages concordant (at 2σ) with isochron ages, with isochrons indicating a trapped argon component within 2σ of atmospheric composition (Figure 7a). In accordance with standard procedure at the Oregon State University lab we accept these plateau ages as the preferred ages. Four samples yielded plateau ages, which failed to overlap (at 2σ) with their isochron ages. The isochrons for these samples indicate excess argon, and the isochron age is preferred (Figure 7b). One sample (2WHLP97) yielded overlapping plateau and isochron ages with a well-developed isochron suggesting excess argon, and the isochron age is preferred for this sample. One sample (148CHLP98; Figure 7c) did not yield a plateau, but all data lie on an isochron indicating excess argon. One sample (145CHLP98) did not yield a three-segment plateau but yielded two precisely determined sequential releases that constitute 56% of the ^{39}Ar released in this experiment. We accept the two-segment plateau age as the preferred age of this sample. The remaining four experiments did not produce reliable crystallization ages. We report integrated ages but do not consider them meaningful age estimates.

[18] The dating results are consistent with known stratigraphic relationships, excepting three basalts from Egli Rim. Samples from two of the lowest lava flows in the section (13WHLP98 and 15WHLP98) yielded ages of 5.58 ± 0.11 and 5.26 ± 0.09 Ma, and a sample from the rim flow (24WHLP98) yielded an age of 5.89 ± 0.12 Ma. The youngest and oldest of these ages are just beyond 2σ of one another. *Hart et al.* [1984] analyzed rim and base samples at Egli Rim by the K-Ar method and also reported a younger age from the base of the section (5.80 Ma rim, 5.21 Ma base). The lower flows are more likely to have been heated or altered, resulting in some argon loss. Alternatively the rim flow could bear excess argon; this is suggested by high ^{40}Ar/^{36}Ar at low ^{39}Ar/^{36}Ar of low- and high-temperature steps excluded from the plateau.

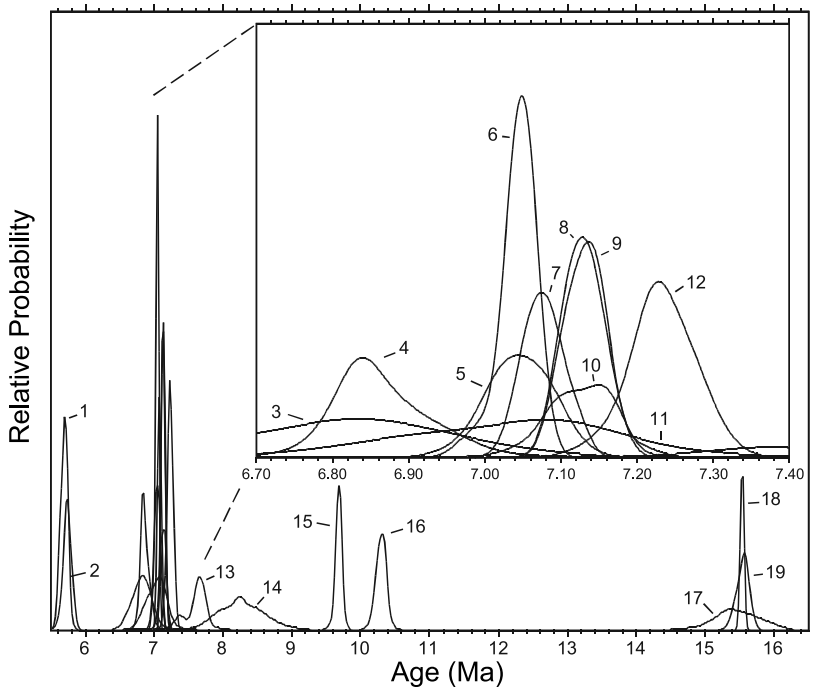

Figure 5. Age-probability spectra for all samples dated by the laser total fusion method. Inset is an enlargement of the interval from 6.7 to 7.4 Ma. The age probabilities are calculated assuming a unit Gaussian error for each analysis, followed by summation across all samples of probabilities within narrow age intervals. Numbers identifying spectra refer to the following samples: 1, HP-91-13 and JR-91-25; 3, HP-91-9; 4, JR-92-56; 5, HP-91-10 (obsidian); 6, HP-91-12; 7, HP-93-4; 8, HP-93-25; 9, HP-93-2; 10, HP-93-13C; 11, HP-91-10 (sanidine); 12, HP-93-16; 13, HP-91-2; 14, DO-93-13; 15, DC-215a; 16, JJ92-5; 17, HP-91-14 (plagioclase); 18, HP-91-14 (sanidine); 19, HP-91-7.

[19] Where the new ages for rhyolitic units are $^{40}Ar/^{39}Ar$ analyses of units previously dated by the K-Ar technique, the new data are typically 10 times more precise and a little older. Ages for the Devine Canyon (9.74 ± 0.02 Ma), Prater Creek (8.41 ± 0.16 Ma), and Rattlesnake Tuffs (7.093 ± 0.015 Ma) have been precisely determined and lie within error of the oldest previously reported ages for these units; previous ages ranged over more than 2 m.y. Morphologically youthful basalts yielded Quaternary ages. Three dacitic centers yielded 15.3–15.7 Ma ages and expand the distribution of known silicic volcanism of middle Miocene age (Figure 1).

[20] One basalt from the lower portion of a section near French Glen, on the west flank of Steens Mountain, yielded an age of 16.68 ± 0.13 Ma. This age coincides, at 1σ, with ages reported to bracket the upper 31 flows of Steens Basalt exposed on Steens Mountain (16.58 ± 0.05 to 16.59 ± 0.02 Ma [*Swisher et al.*, 1990]), indicating that this is a Steens Basalt flow.

5. Discussion of Ages

5.1. Propagation of Rhyolitic Volcanism

[21] New rhyolite ages confirm the contention of *Walker* [1974], *MacLeod et al.* [1975], and *McKee and Walker* [1976] that silicic volcanism is progressively younger to the west along the High Lava Plains. The exception, the Iron Mountain dome (2.89 ± 0.08 Ma), is also confirmed by our results to be much younger than the overall trend [*Walker*, 1974; *MacLeod et al.*, 1975; *McKee and Walker*, 1976].

[22] Figure 8 shows the dated rhyolite occurrences projected to the axis of the HLP. Most of the data from 11 to 5 Ma fall in a field drawn to represent a 2 m.y. duration of silicic volcanism at any point along the trend. The slope of the axis of this field indicates a propagation rate of 33 km/m.y. Projecting this trend westward would miss most of silicic volcanic rocks of the western HLP, and Cascade Range, intersecting only Benham Butte, an imprecisely dated Cascade Range dacite dome [*Fiebelkorn et al.*, 1983]. The current focus of the trend has been postulated to be at Newberry volcano [*Walker*, 1974; *MacLeod et al.*, 1975; *McKee and Walker*, 1976] or South Sister, a Cascade Range volcano [*Hill and Taylor*, 1989]. Extending the trend to either Newberry Volcano or South Sister Volcano reflects a slowing of the propagation rate, with the former requiring the greatest slowing. Projecting the system to South Sister misses all of the domes of the western HLP, so we prefer the interpretation that includes Newberry in the Recent focus, implying a propagation rate of 13 km/m.y. since 5 Ma. Silicic volcanism has been widespread in the western HLP and adjacent Cascades over the last million years (Figure 8). The Three Sisters area is the most productive segment of the Cascades in Quaternary time [*Sherrod and Smith*, 2000], supporting the notion of interaction between the High Lava Plain and Cascade provinces. Helium isotope data for Newberry flank lavas suggest an affinity with the Cascade Range

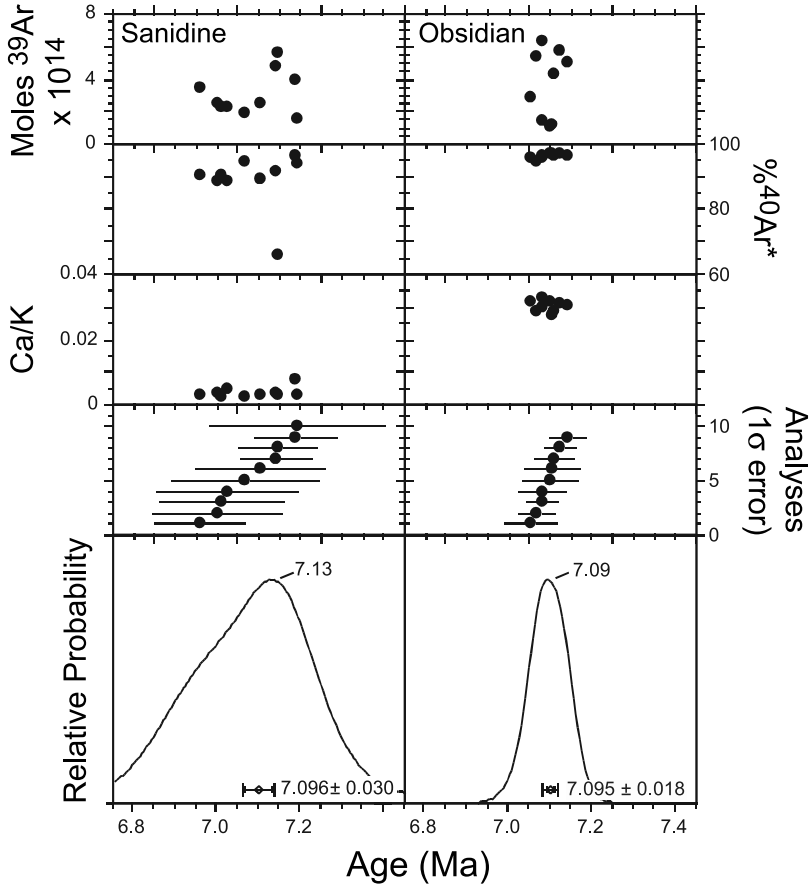

Figure 6. Age-probability diagrams for auxiliary plots of $^{40}Ar/^{39}Ar$ analytical data (moles ^{39}Ar, percent radiogenic ^{40}Ar [^{40}Ar *], Ca/K ratio, and a display of individual analyses) for laser total fusion dating of coexisting obsidian glass and sanidine from sample HP-91-10 collected from Horse Mountain. The mode of each spectrum is shown near the peak of the curves. Error bars near the bottom represent the standard error of the weighted mean, both with (outer ticks) and without (inner ticks) error in J, the neutron fluence parameter.

[*Jordan et al.*, 2000]. We therefore offer that the term "High Lava Plains trend" is less ambiguous than "Newberry trend" or "Newberry hot spot" track [cf. *Humphreys et al.*, 2000; *Christiansen et al.*, 2002].

[23] The age progression across the HLP was first represented as a series of isochrons by *MacLeod et al.* [1975], and this representation continues to be used in most recent literature [e.g., *Humphreys et al.*, 2000; *Christiansen et al.*, 2002]. We have shown that most of the rhyolite age data for the HLP fit in an envelope suggesting a duration of 2 m.y. for silicic volcanism at any given point along the trend. Given this duration of volcanism, isochrons cannot fit all points of one age, as this results in misleading contortions. The isochrons in Figure 3 mark the arrival of volcanism at any point.

5.2. Middle Miocene Silicic Magmatism

[24] We report new ages for three dacite domes, Horsehead Mountain (15.63 ± 0.03 Ma), Little Juniper Mountain (15.65 ± 0.04 Ma), and Jackass Butte (15.34 ± 0.19 Ma). Previous ages of 15–16 Ma for four other silicic domes in the HLP and adjacent northern Basin and Range have been reported (Figure 3; 16.0 ± 0.4 Ma Drum Hill Dome is just south of map area). These middle Miocene silicic domes, however, differ from rhyolites of the HLP age progression in that they are predominantly dacite and rhyodacite-rhyolite, and only rarely high-silica rhyolite [*MacLean*, 1994]. These domes are contemporaneous with widespread ash flow volcanism in southeastern Oregon and north central Nevada (Figure 1), including the McDermitt volcanic field (as summarized by *Pierce and Morgan* [1992]), and expand the westward extent of silicic magmatism of this age.

[25] The middle Miocene episode of silicic volcanism is contemporaneous with the eruption of voluminous flood basalts of the Columbia River basalts (CRB) and Steens Basalt. Many workers interpreted the Steens and CRB eruptions as the result of the head of the Yellowstone plume impinging upon the base of the lithosphere [e.g., *Brandon and Goles*, 1988; *Thompson and Gibson*, 1991; *Geist and Richards*, 1993; *Camp*, 1995; *Hooper*, 1997; *Camp et al.*, 2003]. *Pierce and Morgan* [1992] interpret widespread silicic volcanism at this time to also reflect the plume head phase of the Yellowstone plume. If this is the case, then the presence of middle Miocene silicic volcanic rocks spanning ~130 km, across more than half the length of the HLP,

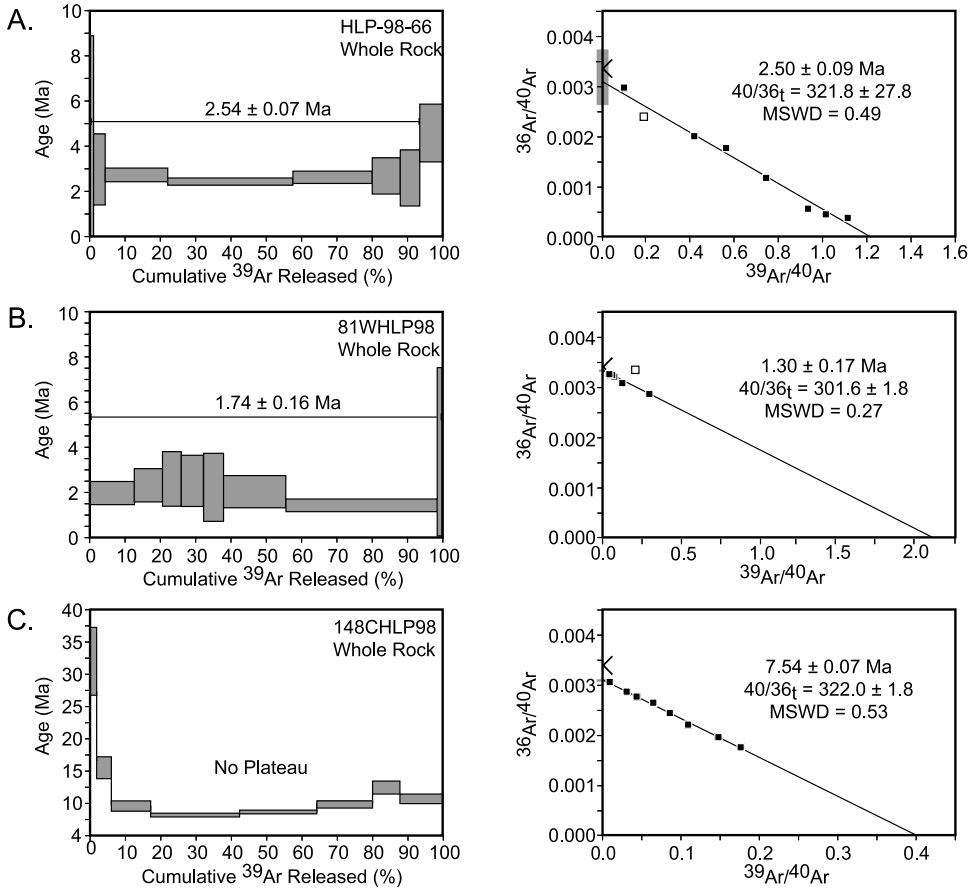

Figure 7. Representative plateau and inverse isochron plots for incremental heating analyses performed at Oregon State University. Segments on plateau plots are shown with 2σ uncertainty. On isochron plots, shaded squares are data used to determine isochrons; right pointing arrowhead indicates atmospheric ratio (1/295.5); and gray range indicates 1σ uncertainty on the $^{36}Ar/^{40}Ar$ intercept. (a) A well-developed plateau and a concordant isochron with intercept within 2σ of atmospheric value. Plateau age is accepted age. (b) Plateau and isochron with $^{36}Ar/^{40}Ar$ intercept beyond 2σ of atmospheric ratio. Isochron age is accepted age. (c) No plateau developed, but a good isochron indicates excess ^{40}Ar. Isochron age is accepted age.

indicates the minimum extent of this plume head was ~400 km in radius if the plume was centered in south central Idaho, as argued below.

5.3. Timing of Basaltic Volcanism

[26] The basalts of the HLP have no clear spatial-temporal trend (Figure 8); basalts as old as 7.75 Ma are found in the western HLP. However, we observe other features in the age distribution. The oldest post-Steens basalts dated in the east are older than those in the west, although this may simply reflect the general paucity of deep exposure in the west. In the northern Basin and Range, there is a coarse westward progression in the age of cessation of basaltic volcanism, with no Pliocene basalts east of ~121°W (within the map area). Quaternary basalts are limited to the axis of the HLP, and are sparse in the central HLP (Figure 3). There is some indication of episodes of province-wide basaltic volcanism, with possible episodes of increased activity at 7.5–7.8, 5.3–5.9, and 2–3 Ma (Figure 8). In the eastern HLP, there may be a hiatus in activity between 5 and 3 Ma, while in the western HLP, basaltic volcanism is more continuous (Figure 8).

[27] The 7.5–7.8 Ma episode is the most robust of the suggested episodes. Eight of the $^{40}Ar/^{39}Ar$ basalt ages reported here overlap within 2σ with an average of 7.60 Ma. These samples span nearly 200 km of the HLP, suggesting a major regional event, perhaps related to an early phase of activity on the Brothers Fault Zone. We also note that the 7.6 Ma event preceded a widespread and relatively voluminous episode of silicic volcanism (~7.1 Ma; focused in the central HLP) by about half a million years. The timing of this event also corresponds with the initiation of the ongoing High Cascades phase of Cascades volcanism and tectonism (estimated initiation age of ~7.4 Ma [*Priest*, 1990]). These tectonomagmatic events in the HLP and Cascade Arc coincide with a change in the azimuth of motion of the Pacific plate to a more northerly direction [*Atwater and Stock*, 1998]. This change would have caused more northerly motion of the Juan de Fuca plate and therefore more oblique subduction. The margin-parallel component of oblique subduction gives rise to

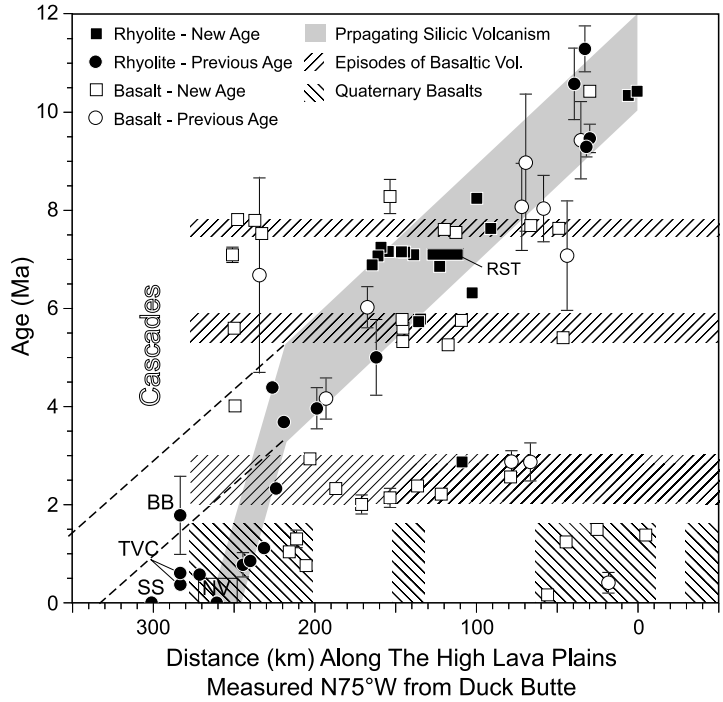

Figure 8. Plot of published and new rhyolite and basalt ages versus distance along the HLP trend. Data are projected N15°E or S15°W to the axis of the N75°W trending belt of Quaternary HLP basalts. Error bars indicate 1σ error. RST is the Rattlesnake Tuff. Sources of previous ages are those cited in Figures 3 and 4 plus ages for silicic tuffs erupted from the Tumalo volcanic center (TVC) from *Sarna-Wojcicki et al.* [1989]. Also shown are silicic lavas erupted at Newberry Volcano (NV), South Sister (SS), and Benham Butte (BB). The shaded field indicates the silicic age progression as interpreted here: 33 km/m.y. from 11–5 to 5 Ma and 13 km/m.y. from 5 Ma to Recent, with a 2 m.y. duration of rhyolitic volcanism at any point along the trend. The diagonally ruled fields depict the episodes of province-wide enhanced basaltic volcanic events including the mapped distribution of Quaternary basalts.

shear tractions that cause block rotation and extension in the overriding plate [*DeMets*, 1995]. This process links deformational and magmatic events in the HLP to the general transition of western North America from a subduction-dominated margin to a transtensional margin.

[28] The 5.3–5.9 Ma episode is preserved by basalts mostly in the central HLP and northern Basin and Range, including Egli and Burma Rims along the extreme northern margin of the Basin and Range. The 2–3 Ma episode is suggested by widely distributed ages along the axis of the High Lava Plains. Quaternary basalts are present along about 50% of the length of the HLP, mostly near the eastern and western ends of the province. Late Quaternary basalts are restricted to Newberry volcano, the area immediately east of Newberry, and Diamond Craters in the eastern HLP. Quaternary volcanism of the HLP can be viewed as an episode, equivalent to the earlier proposed episodes and, perhaps viewed as a continuation of the province-wide volcanism initiated between 2 and 3 Ma.

6. Regional Relationships

6.1. High Lava Plains Magmatism and Regional Structure

[29] Basaltic, and less commonly silicic, vent systems are aligned parallel to local fault geometries. An example is the East and Four Craters lava fields in the western HLP. The four cinder cones of the Four Craters field form a northwest alignment that projects to the vent complex of the East lava field. Although not contiguous on the surface, identical distinctive compositions of the East and Four Craters lava fields indicate that they are probably linked by dikes in the shallow subsurface, and the northwest trending vent alignment is parallel to local fault patterns. These relationships indicate structural/tectonic control of magma conduit systems in the upper crust.

[30] An additional link between magmatism and development of geologic structure is suggested by the observation that the system of closely spaced northwest trending faults that includes the Brothers Fault Zone dies out within 20 km to the north of the belt of silicic volcanism and the belt of Pliocene and younger basalts of the HLP (Figure 3). This observation suggests a genetic relationship for which there are two hypotheses: (1) magmatic weakening of the crust was responsible for the distribution of the fault system; or (2) faulting was responsible for localizing volcanism or even magma genesis.

[31] It has been proposed that age progressive volcanism of the HLP could be explained by propagation of a shear zone (presumably the Brothers fault zone) across the HLP [*Christiansen and McKee*, 1978; *Christiansen et al.*, 2002]. Comparison of faulting of rocks of similar age in the western and eastern HLP allows a test of the hypothesis that the Brothers Fault Zone has propagated across the HLP,

possibly driving age progressive magmatism. Qualitative examination of faults cutting 7–8 Ma rocks and 2–3 Ma rocks across the HLP reveals that the spacing and apparent displacement are not grossly different in the east and the west in units of similar age. This suggests that the Brothers Fault Zone has been active across the entire HLP since at least ~8 Ma. Preliminary GIS analysis of fault patterns in domains of rocks of known age across the HLP confirms that faulting has not propagated, and suggests a maximum of just over 1% extension in ~8 Ma [*Jordan*, 2004], a rate too slow to drive magma genesis by adiabatic decompression.

6.2. The High Lava Plains, Yellowstone–Snake River Plain System, and Middle Miocene Magmatism

[32] Spatial, temporal, and petrologic characteristics suggest a link between the HLP and YSRP trends, and middle Miocene flood basalt volcanism (Columbia River basalts and Steens Basalts). Both the HLP and YSRP trends emerge from the axis of middle Miocene flood basalt vents (Figure 1). The area from which the trends emerge is also a broad region of middle Miocene dacitic-rhyolitic volcanism that was contemporaneous with the flood basalts. Both the HLP and YSRP trends became well defined at about 10–12 Ma. The trends propagate at similar rates (YSRP ~40 km/m.y., HLP 33 km/m.y.) from this time until the slowdown of the HLP at ~5 Ma. Both trends are also characterized by bimodal volcanism, with basalts that are not age progressive. Pliocene and younger basalts are found along the lengths of both trends, and in the intervening Owyhee Plateau. Basalts in both trends are predominantly tholeiites, though the YSRP basalts are more isotopically evolved and more enriched in incompatible trace elements.

[33] As has been described by *Pierce and Morgan* [1992] and *Smith and Braille* [1994], significant differences in the HLP and YSRP include the types and volumes of silicic eruptive products, and structural setting. HLP rhyolites were mostly erupted as domes with eruptive volumes generally <1 km^3. The YSRP silicic rocks are mostly tuffs, and YSRP ignimbrites are typically of much greater volume, thousands of cubic kilometers versus hundreds of cubic kilometers for the larger HLP tuffs. It has been stated that both trends are at the northern margin of the Basin and Range [e.g., *Christiansen et al.*, 2002]. However, while the HLP is along the northern margin of the Basin and Range, significant Basin and Range extension continues north of the YSRP [*Rodgers et al.*, 2004]. The two provinces have developed on crust of vastly different history and composition. The HLP lies on Paleozoic and Mesozoic oceanic and arc terranes accreted to North America in the Mesozoic, and the YSRP developed on the Precambrian craton of North America, the western margin of which is marked by the Sr isotope discontinuity (Figure 1).

7. Tectonic Models

7.1. Evaluation of Previous Models for the High Lava Plains

[34] Previously proposed models for the origin of the High Lava Plains have called upon processes active in the adjacent provinces, including (1) extension of the Basin and Range [*Christiansen and McKee*, 1978; *Christiansen et al.*, 2002], (2) subduction-related processes in the back arc of the Cascade arc [*Carlson and Hart*, 1987], and (3) mantle plume processes of the YSRP and Columbia River basalts [*Draper*, 1991] or, more generally, (4) the aftereffects of emplacement of the middle Miocene large igneous province, regardless of its origin [*Humphreys et al.*, 2000].

[35] *Christiansen et al.* [2002] attribute the westward propagation of silicic magmatism to enhanced extension at the northern margin of the Basin and Range that propagated with extensional widening of the province. *Christiansen* [1993] proposed that crustal melting may have been driven by basal lithospheric shear melting with dynamic feedback. We concur that faulting and tectonic stress have exerted significant control on the transmission of magma into and through the crust. However, as discussed above, Brothers Fault Zone and associated faults did not propagate during the interval in which rhyolitic volcanism migrated. Further, this model fails to provide a clear mechanism to initiate mantle melting that drove the HLP magmatic system. Preliminary results of a structural study suggest deformation in the HLP was minor, probably about 1% extension over ~8 m.y., insufficient to drive a magmatic system by adiabatic decompression.

[36] *Carlson and Hart* [1987] focused on the development of middle Miocene flood basalt volcanism and developed a model in which steepening of the subducted slab under the Cascade arc caused considerable extension in the overriding plate and mantle upwelling at the craton margin. They envisioned the area of the HLP as an area of crustal genesis analogous to an oceanic back arc basin. In this context, migrating silicic volcanism of the HLP marked the growth of the region of extension and crust formation. At the time this model was proposed large magnitudes of extension seemed to be required by the interpretation that paleomagnetic results from the Oregon Coast Range reflected clockwise block rotation of the Coast Range and Cascades [e.g., *Magill and Cox*, 1981]. *Wells and Heller* [1988] propose that these paleomagnetic results may, in part, be accounted for by the rotation of blocks within the Coast Range, eliminating the need for the substantial extension. Further, the model of *Carlson and Hart* [1987] does not account for the relationship with the YSRP trend which we find compelling.

[37] The model of *Draper* [1991] attributes the HLP trend to entrainment of Yellowstone plume head material in subduction-induced counter flow. This is consistent with the similarity between the HLP propagation rate and the plate convergence rate. However, this model would predict age propagation of basaltic volcanism across the HLP, which has not occurred since at least 7–8 Ma. The model is also at odds with current models of plume head dynamics in which plumes flatten as they approach the lithosphere [*Griffiths and Campbell*, 1991] and are emplaced across areas as large as 2000 km diameter in periods of a few million years [*Duncan et al.*, 1997].

[38] The model of *Humphreys et al.* [2000] makes no comment on the origin of middle Miocene flood basalt volcanism but suggests that decompression of asthenosphere flowing around the buoyant viscous residuum of this event caused HLP and YSRP volcanism. In this model the HLP trend is caused by westward flow in the subduction-induced counter flow cell, and YSRP volcanism reflects

plate motion. The broad similarity of the HLP propagation rate, at least prior to 5 Ma, to the convergence rate at the Cascadia subduction zone supports this model in a general way. However, the HLP and YSRP trends diverge from the Owyhee Plateau, not the area that was the source of the bulk of the middle Miocene flood basalts (northeast Oregon and southeast Washington). Also, if the craton was underlain by thicker lithosphere than the accreted terranes, then the residuum would have to have been thicker than the difference in lithospheric thickness (perhaps 50–100 km) in order to have maintained the relief around which flow could have caused propagating magmatism of the YSRP.

7.2. Plume Model for the Yellowstone–Snake River Plain System

[39] Because the evidence for a link between the HLP and YSRP is formidable, it is relevant to consider the validity and implications of the mantle plume model for the origin of the YSRP. The interpretation that the YSRP system is the result of a mantle plume, and that the Columbia River and Steens Basalts represent the initiation of this plume has been developed and supported by many workers [e.g., *Brandon and Goles*, 1988; *Pierce and Morgan*, 1992; *Smith and Braille*, 1994; *Hooper*, 1997; *Camp et al.*, 2003]. However, the differences between the YSRP and oceanic hot spot systems have led to considerable debate as to the applicability of the simple plume model for the YSRP [e.g., *Hamilton*, 1989; *Christiansen et al.*, 2002].

[40] If the YSRP trend reflects plate motion over a stationary hot spot, generally interpreted as a mantle plume, the propagation rates (track lengths) are in conflict with North American plate motion estimated by global plate motion models (Figure 1). The misfit is most pronounced in the older portion of the trend, as generally depicted, that extends from the Snake River Plain across the Owyhee Plateau to the McDermitt volcanic field (Figure 1). *Smith and Braille* [1994] reconcile this contradiction by postulating that extension along the axis of the Snake River Plain has exaggerated the apparent rate of volcanic migration. However, *Rodgers et al.* [1994, 2004] estimated extension immediately south of the Snake River Plain to be ~20%, nowhere close to the 50–300% required to reconcile observed rates of volcanic propagation to the plate motion models.

[41] Another potential explanation for of this contradiction is to invoke the relative motion of hot spots. However, when the model of *Steinberger and O'Connell* [2000], which successfully predicts the relative motion of Pacific hot spots, is applied, the prediction is for a trend that is not much longer and with a considerably more easterly azimuth than observed for the YSRP [*Steinberger*, 2000]. If Columbia River and Steens Basalt magmatism is interpreted to reflect the initiation of the plume, then the model of *Steinberger and O'Connell* [2000] also predicts a shorter track than observed as they suggest that the upper plume conduit would be dragged with the plate for the first 5 m.y.

[42] The link between the YSRP and middle Miocene flood basalts is complicated by the off-track position of the Columbia River basalt vents that account for the bulk of middle Miocene flood basalt volcanism. Models have been proposed that explain this as the result of either deflection of the plume by the subducted slab [*Geist and Richards*, 1993; *Pierce et al.*, 2000], plume-lithosphere interaction [*Thompson and Gibson*, 1991; *Camp*, 1995], or lateral propagation of dikes [*Takahahshi et al.*, 1998]. *Thompson and Gibson* [1991] proposed that the off-track position of Columbia River basalt vents could be explained by melting being focused at the point where plume material was emplaced at shallow depths, under accreted terranes. This model explains volcanism at locations away from the plume center and therefore also offers an explanation for the track length problem. Both plume head and conduit material could have flowed westward on basal lithospheric topography [e.g., *Sleep*, 1996] from under the thick craton to the accreted terranes, focusing magmatism at the craton margin, in a processes analogous to plume-ridge interaction [e.g., *Ito et al.*, 2003].

7.3. A Working Model for High Lava Plains Magmatism

[43] We propose a model for the development of the High Lava Plains that explains its location at the margin of the Basin and Range province, the age-progressive silicic volcanism, and the pulsatory mafic volcanism. Through combinations and variations of existing models, we propose a scenario in which a mantle plume interacted with the complex lithospheric structure and tectonic history of the western U.S. to result in HLP magmatism (Figure 9).

[44] First, we propose impingement of a mantle plume centered under the central Snake River Plain (Figure 9). Our model differs from existing plume models in that the center of impingement is not under the McDermitt caldera region [cf. *Smith and Braille*, 1994; *Camp*, 1995]. Instead, we propose impingement consistent with plate motion reconstructions (Figure 1) and thus also with track length for YSRP. The head of the rising plume flattened as it approached the lithosphere, as modeled by *Griffiths and Campbell* [1991]. The emplacement of even a modest sized (diameter of ~1000 km) flattened plume head centered under southern Idaho affected the mantle under the entire HLP, which played a role in subsequent magmatism.

[45] The flattening, spreading, and internally convecting plume head (see the model of *Griffiths and Campbell* [1991]) affected a vast region of the mantle with decreasing intensity from the center to the edges. It also mixed with and displaced ambient mantle. Where it flowed up the lithospheric boundary between the craton and accreted terranes (0.706 line), decompression-induced melting produced a pulse of voluminous mafic dikes and flows of the northern Nevada Rift, Steens Basalts, Columbia River basalts between 17 and 15 Ma (Figure 9), similar to the model of *Thompson and Gibson* [1991]. Away from the craton margin, mafic magmatism caused by the plume head was less intense, but plume head emplacement did induce crustal magmatism as reflected by widespread middle Miocene silicic volcanism in the northern Basin and Range, Owyhee Plateau, and HLP between 16 and 14 Ma [e.g., *Pierce and Morgan*, 1992; *Hooper et al.*, 2002; this study]. Surface expression of the plume head on the Precambrian craton was dampened by the thick lithosphere.

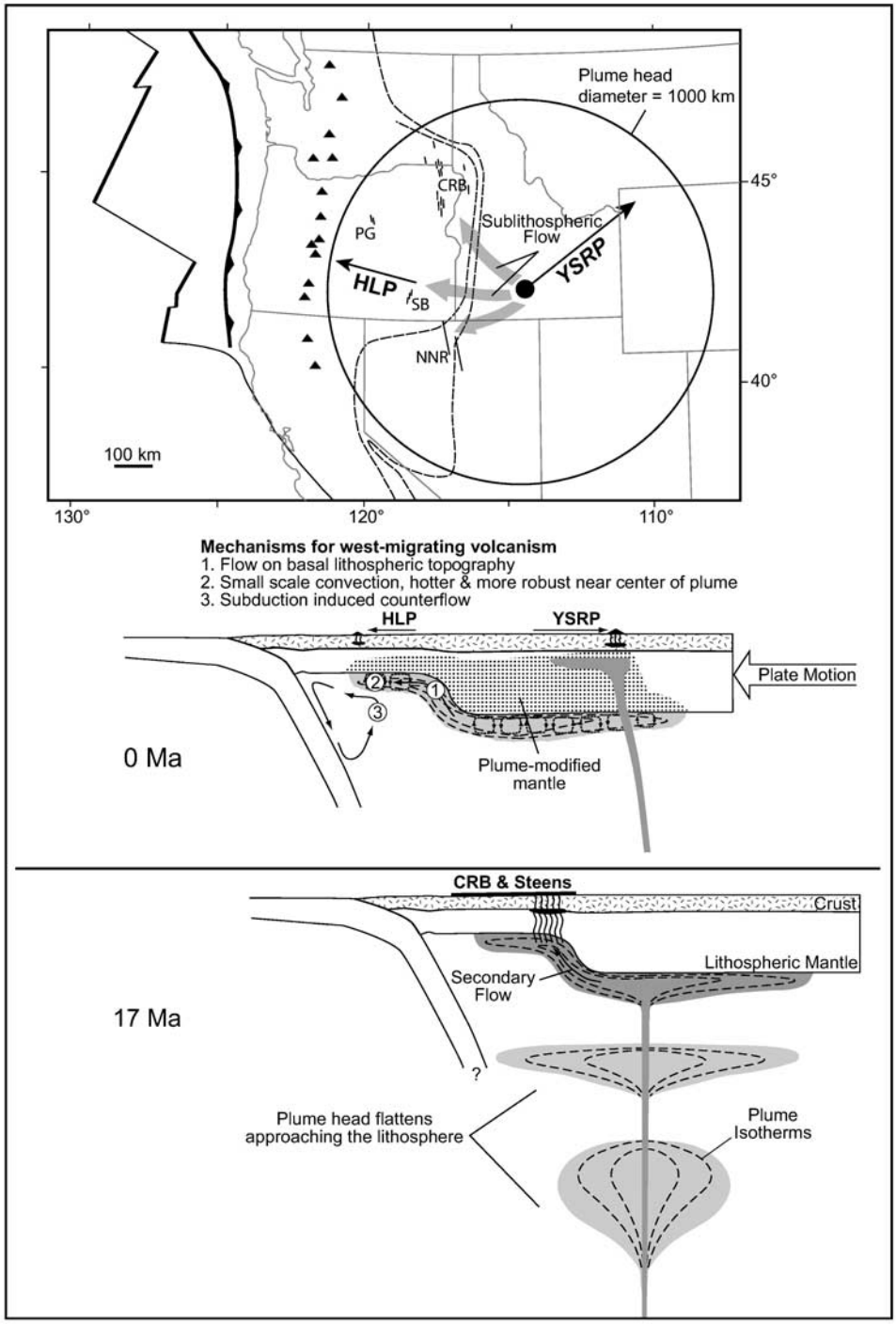

Figure 9. Cartoon depicting the model envisioned to explain the distribution of middle Miocene basaltic vents and trends of migrating silicic volcanism of the HLP and YSRP. Many map features shown are as explained in Figure 1; PG, dikes of the Picture Gorge Basalts.

[46] In our model, age-progressive silicic volcanism from about 12 Ma to Recent along the YSRP is the expression of the plume track. The length of this portion of the YSRP trend is consistent with that predicted by global plate motion models (Figure 1).

[47] The part of the plume head model essential to the HLP trend is that the underlying mantle was modified by the event, consistent with the generally uniform, and slightly westward decreasing $^{87}Sr/^{86}Sr$ isotopic composition of middle Miocene and late Miocene basalts of the region (Figure 10). It seems likely that the crust was also modified by underplating of basalts of that episode.

[48] Superimposed on the regional lithospheric structure is the location of the persistent structural margin of the

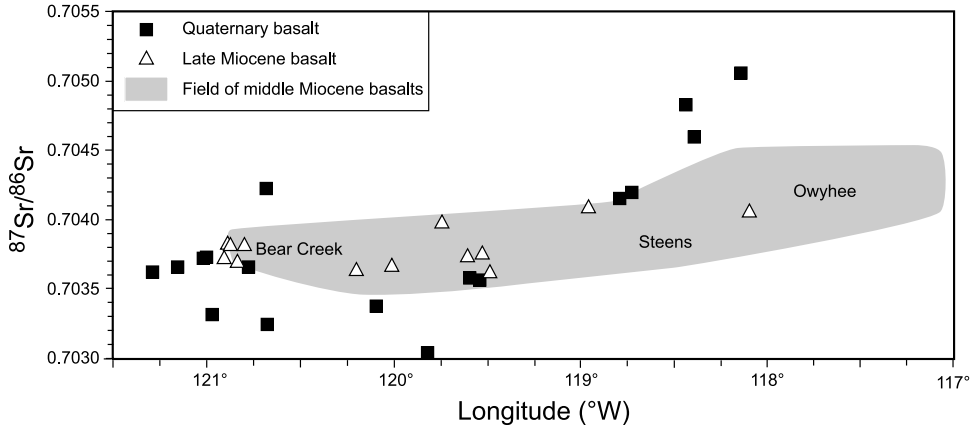

Figure 10. Initial Sr isotope composition of HLP basalts [from *Jordan*, 2001; *Jordan et al.*, 2002b]. Shaded area shows range of middle Miocene basalts immediately east and north of the HLP based on data from *Carlson and Hart* [1987] and *Brandon and Goles* [1995].

Basin and Range that provides a transtensional regime for magma conduits to the surface and so engendered volcanism of the HLP. The province is thus sensitive to magma-inducing disturbances in the mantle that are not expressed where crustal transit of magma is inhibited. In this context, the ~7.6 Ma pulse of basaltic volcanism of the HLP reflects changes in tectonic convergence geometry at the plate margin [*Atwater and Stock*, 1998]. Also, the abundance of age-progressive high-silica rhyolite silicic volcanism, which defines the HLP tend, is greatest along the HLP, but contemporaneous volcanism extends to the south into the northern Basin and Range.

[49] What, then, causes the age progression of the silicic volcanism of the HLP? Within the context of the above scenario there are two broad categories of plume-related processes that could have been manifested in an age progression: (1) the delayed effects of plume head emplacement; and (2) westward flow of hot plume material, beyond that emplaced by the plume head, under the HLP.

[50] Hotter and more actively convecting [*Griffiths and Campbell*, 1991] plume head material would have been emplaced under the eastern (closer to the plume center) than the western HLP. The eruption of silicic volcanics in the eastern half of the HLP contemporaneous with flood basalt volcanism may reflect this. The amount of time required for the crust to incubate for subsequent magma genesis by underplating and injection by mafic magmas would have been greater in the west than the east, producing an age progression. The absence of an age-progressive wave in other sectors of the plume head reflects an absence of thin and extended crust. This process could explain the migration of silicic volcanism across the HLP and the northwesternmost Basin and Range as a wave. It could also explain the general decline in volume of silicic volcanics through time across the HLP (tuffs >100 km^3 in the eastern HLP only). A broadly similar processes was interpreted in the Paraná flood basalt province in South America where *Garland et al.* [1996] interpret an age progression in lithospherically derived magmas across a distance of >500 km over a period of ~9 m.y. as the result of heating of the lithosphere by the head of a mantle plume.

[51] Westward flow of plume material is an alternative or complementary process that could have driven west migrating silicic volcanism. Westward flow could have been driven by either continued flow along the slope on the base of the lithosphere at the craton margin, or subduction-induced counter flow [cf. *Draper*, 1991; *Humphreys et al.*, 2000]. We favor a continued role for basal lithospheric topography because it could account for the slowing of propagation and decreasing volume of silicic magmatism as results of the attenuation of flow at some distance from the topographic gradient (craton margin) driving flow.

[52] Time-space patterns in Sr isotope composition of HLP basalts are also consistent with our model (Figure 10). Since the late Miocene, the character of the source of HLP basaltic magmas has shifted from the spatially homogeneous source that we interpret to be the plume head to more variable sources; more depleted in the west and more enriched in the east (Figure 10). The depleted values in the west may reflect a greater contribution from a depleted asthenospheric source, possibly related to back arc processes. The eastern HLP is west of the 0.704 line (Figure 1), yet the Quaternary basalts of the eastern HLP reach $^{87}Sr/^{86}Sr$ of >0.705. This suggests influx of an enriched component, perhaps thermomechanically eroded cratonic lithosphere that was brought westward in sublithospheric flow.

[53] HLP magmatism can be understood as the indirect consequence of plume head emplacement or subsequent flow of plume material. Either way, we suggest that the HLP trend is more readily explained by a plume-related model than as the product of Basin and Range extension alone. The HLP has not undergone enough structural extension to account for upwelling and an extension model cannot readily account for decease in volcanism to the west. Nevertheless, the localization of magmatism to the HLP is dependent on structural context. Basaltic and rhyolitic volcanism are both more focused in the HLP than the Basin and Range immediately to the south, suggesting that the transtensional structural boundary represented by the northern margin of the Brothers Fault Zone is important in allowing magmas to intrude and transit through the crust.

Table A1. Sample Locations

Sample	Latitude, °N	Longitude, °W	Laboratory/Technique[a]
DC-215a	44.1666	118.9931	BGC/LTF
DO-93-13	43.2506	119.2603	BGC/LTF
HP-91-2	43.5531	119.2497	BGC/LTF
HP-91-7	43.1597	119.8936	BGC/LTF
HP-91-9	43.2366	120.1144	BGC/LTF
HP-91-10	43.1775	120.1217	BGC/LTF
HP-91-12	43.8886	120.0454	BGC/LTF
HP-91-13	43.5086	119.7400	BGC/LTF
HP-91-14	43.2572	120.1658	BGC/LTF
HP-93-2	43.4327	119.8533	BGC/LTF
HP-93-4	43.3942	119.8264	BGC/LTF
HP-93-13C	43.3528	119.8653	BGC/LTF
HP-93-16	43.2403	120.1083	BGC/LTF
HP-93-25	43.2517	120.0397	BGC/LTF
JJ92-5	43.142	118.146	BGC/LTF
JR-91-25	43.4837	119.7605	BGC/LTF
JR-92-56	43.4771	119.5317	BGC/LTF
HP-91-4	43.4894	119.3019	BGC/IH
HP-91-5	43.2582	119.4452	BGC/IH
HP-91-11	43.2572	120.1658	BGC/IH
JJ92-1	43.173	118.151	BGC/IH
JJ92-20	43.141	118.148	BGC/IH
PC-1	43.681	119.095	BGC/IH
1WHLP99	43.9058	121.0060	OSU/IH
2WHLP97	43.9220	121.0048	OSU/IH
8WHLP97	43.9281	121.0051	OSU/IH
13WHLP98	43.0913	120.8384	OSU/IH
15WHLP98	43.0913	120.8375	OSU/IH
24WHLP98	43.0907	120.8381	OSU/IH
25WHLP98	43.3338	120.6711	OSU/IH
30WHLP98	43.5535	121.2917	OSU/IH
48WHLP98	43.7925	120.8550	OSU/IH
74WHLP98	43.9575	120.8396	OSU/IH
76WHLP98	43.7221	120.7536	OSU/IH
81WHLP98	43.6133	120.6870	OSU/IH
103WHLP98	43.1157	120.9492	OSU/IH
123WHLP98	43.7284	120.4059	OSU/IH
128WHLP98	43.8174	120.4790	OSU/IH
130WHLP98	43.6538	120.1027	OSU/IH
138WHLP98	43.4659	119.8200	OSU/IH
145CHLP98	43.4685	119.5532	OSU/IH
148CHLP98	43.2466	119.5299	OSU/IH
HBA-13.5	43.5917	119.4483	OSU/IH
HBA-3	43.5567	119.4283	OSU/IH
HLP-98-6a	43.1265	120.3913	OSU/IH
HLP-98-12	43.1261	120.3898	OSU/IH
HLP-98-24	42.5711	119.6512	OSU/IH
HLP-98-32	43.0373	118.9458	OSU/IH
HLP-98-33	43.0570	118.9583	OSU/IH
HLP-98-35	42.9904	118.8666	OSU/IH
HLP-98-40	43.1316	118.6601	OSU/IH
HLP-98-42	43.1925	118.8192	OSU/IH
HLP-98-54	43.2270	118.4755	OSU/IH
HLP-98-59	43.1397	118.4443	OSU/IH
HLP-98-66	43.4467	119.0035	OSU/IH
HP-33	43.0930	119.9362	OSU/IH
JR-91-21	43.4750	119.7200	OSU/IH

[a]BGC, Berkeley Geochronology Center; LTF, laser total fusion; IH, incremental heating; OSU, Oregon State University.

The HLP is therefore best understood as a result of both plume and regional tectonic processes.

8. Conclusions

[54] Our new $^{40}Ar/^{39}Ar$ ages (laser total fusion, laser incremental heating, and furnace incremental heating) for 24 rhyolitic units of the High Lava Plains of central and southeastern Oregon confirm and refine the previous interpretation that ages of silicic volcanism are progressively younger to the west. The rate of propagation of silicic volcanism was ~33 km/m.y. from 10 to 5 Ma and slowed to ~13 km/m.y. from 5 Ma to Recent. The volumetric output of silicic volcanism also declined with time. Our new $^{40}Ar/^{39}Ar$ ages for 34 basaltic units show that basaltic volcanism has occurred across the province since the middle-late Miocene with a province-wide event at 7.5–7.8 Ma and less robust events at 5.3–5.9 Ma, and 2–3 Ma, the latter event possibly continuing to the present.

[55] The HLP trend crudely mirrors the northeast progression of silicic volcanism of the Snake River Plain to the Yellowstone Plateau. We consider these trends related because they originate from the axis of middle Miocene flood basalt volcanism and a region of diffuse silicic volcanism. Both age-progressive trends become organized between 12 and 10 Ma, both are bimodal (basalt and high-silica rhyolite), and a band of Pliocene and younger basaltic volcanism is continuous across both trends. We interpret magmatism of the HLP to be largely the result of the emplacement of the head of the Yellowstone plume under the area, and interactions between the plume, plume head, and the complex lithosphere structure and tectonic history of the Pacific Northwest. Rather than viewing the HLP trend as contradicting the mantle plume model for the Yellowstone-Snake River Plain trend and middle Miocene flood basalts, we suggest that the HLP trend is itself best understood as a consequence of plume processes coupled with transtensional tectonics of western North America.

Appendix A

[56] The locations for samples analyzed in this study are given in Table A1.

[57] **Acknowledgments.** This study benefited from collaboration with Dave Graham, Martin Streck, Jenda Johnson, Jim MacLean, and Eva Rasdal. Some samples were collected by Martin Streck and Jenda Johnson. We are grateful to Lew Hogan and John Huard for their assistance in the geochronology lab at Oregon State University. Coauthors' discussions with Dave Rodgers, Bill Hart, Bob Christiansen, Gillian Foulger, Ed Taylor, John Dilles, Jeffrey Lee, and Andrew Meigs helped us to refine our perspectives on the High Lava Plains. We also appreciate the input of participants in the 2002 GSA Cordilleran Section field trip to the High Lava Plains. Jordan thanks the NSF RIDGE program for funding his participation in the 2000 Iceland Summer School focused on plume-ridge interactions. This manuscript benefited from critical reviews by Bill Hart and an anonymous reviewer and from comments from the Associate Editor, Bruce Nelson. This work was supported by the National Science Foundation (EAR-9220500 to Grunder, EAR-9218879 to Deino, and EAR-9725166 to Grunder, Duncan, and Dave Graham) and by a student research grant from the Geological Society of America to Jordan.

References

Armstrong, R. L., W. P. Leeman, and N. E. Malde (1975), K-Ar dating, Quaternary and Neogene rocks of the Snake River Plain, Idaho, *Am. J. Sci.*, *275*, 225–251.

Atwater, T., and J. Stock (1998), Pacific-North America plate tectonics of the Neogene southwestern United States; an update, *Int. Geol. Rev.*, *40*, 375–402.

Brandon, A. D., and G. G. Goles (1988), A Miocene subcontinental plume in the Pacific Northwest: Geochemical evidence, *Earth Planet. Sci. Lett.*, *88*, 273–283.

Brandon, A. D., and G. G. Goles (1995), Assessing subcontinental lithospheric mantle sources for basalts: Neogene volcanism in the Pacific Northwest, USA as a test case, *Contrib. Miner. Petrol.*, *121*, 364–379.

Camp, V. E. (1995), Mid-Miocene propagation of the Yellowstone mantle plume head beneath the Columbia River basalt source region, *Geology*, *23*, 435–438.

Camp, V. E., M. E. Ross, and W. E. Hansen (2003), Genesis of flood basalts and Basin and Range volcanic rocks from Steens Mountain to the Malheur River Gorge, Oregon, *Geol. Soc. Am. Bull.*, *115*, 105–128.

Carlson, R. W., and W. K. Hart (1987), Crustal genesis on the Oregon Plateau, *J. Geophys. Res.*, *92*, 6191–6206.

Christiansen, R. L. (1993), The Yellowstone hot spot: Deep mantle plume or upper mantle melting anomaly?, *Eos Trans AGU*, *76*, Fall Meet. Suppl., 602.

Christiansen, R. L., and E. H. McKee (1978), Late Cenozoic volcanic and tectonic evolution of the Great Basin and the Columbia intermontane regions, in *Cenozoic Tectonics and Regional Geophysics of the Western Cordillera*, edited by R. B. Smith and G. P. Eaton, *Mem. Geol. Soc. Am.*, *152*, 283–311.

Christiansen, R. L., G. R. Foulger, and J. R. Evans (2002), Upper-mantle origin of the Yellowstone hotspot, *Geol. Soc. Am. Bull.*, *114*, 1245–1256.

DeMets, C. (1995), Plate motions and crustal deformation, *U.S. Natl. Rep. Int. Union Geod. Geophys.*, *1991–1994*, *Rev. Geophys.*, *33*, suppl., 365–369.

Diggles, M. F., J. E. Conrad, and G. S. Soreghan (1990), Geologic map of the Diablo Mountain Wilderness Study Area, Oregon, *U.S. Geol. Surv. Misc. Field Stud. Map*, *MF-2121*.

Draper, D. S. (1991), Late Cenozoic bimodal magmatism in the northern Basin and Range province in southeastern Oregon, *J. Volcanol. Geotherm. Res.*, *47*, 299–328.

Duncan, R. A., and L. G. Hogan (1994), Radiometric dating of young MORB using the ^{40}Ar-^{39}Ar incremental heating method, *Geophys. Res. Lett.*, *21*, 1927–1930.

Duncan, R. A., and M. A. Richards (1991), Hotspots, mantle plumes, flood basalts, and true polar wander, *Rev. Geophys.*, *29*, 31–50.

Duncan, R. A., P. R. Hooper, J. Rehacek, J. S. Marsh, and A. R. Duncan (1997), The timing and duration of the Karoo igneous event, southern Gondwana, *J. Geophys. Res.*, *102*, 18,127–18,138.

Ernst, W. G. (1988), Metamorphic terranes, isotopic provinces, and implications for crustal growth of the western United States, *J. Geophys. Res.*, *93*, 7634–7642.

Fiebelkorn, R. B., G. W. Walker, N. S. MacLeod, E. H. McKee, and J. G. Smith (1983), Index to K-Ar age determinations for the State of Oregon, *Isochron West*, *37*, 3–60.

Fleck, R. J., J. F. Sutter, and D. H. Elliott (1977), Interpretation of discordant ^{40}Ar/^{39}Ar age-spectra of Mesozoic tholeiites from Antarctica, *Geochim. Cosmochim. Acta*, *41*, 15–32.

Garland, F. E., S. P. Turner, and C. J. Hawkesworth (1996), Shifts in the source of the Paraná basalts through time, *Lithos*, *37*, 223–243.

Geist, D., and M. Richards (1993), Origin of the Columbia Plateau and Snake River Plain: Deflection of the Yellowstone plume, *Geology*, *21*, 789–793.

Griffiths, R. W., and I. H. Campbell (1991), Interaction of mantle plume heads with the Earth's surface and onset of small-scale convection, *J. Geophys. Res.*, *96*, 18,295–18,310.

Gripp, A. E., and R. G. Gordon (2002), Young tracks of hotspots and current plate velocities, *Geophys. J. Int.*, *150*, 321–361.

Hamilton, W. B. (1989), Crustal geologic processes of the United States, in *Geophysical Framework of the Continental United States*, edited by L. C. Pakiser and W. D. Mooney, *Mem. Geol. Soc. Am.*, *172*, 743–781.

Hart, W. K., and R. W. Carlson (1987), Tectonic controls on magma genesis and evolution in the northwestern United States, *J. Volcanol. Geotherm. Res*, *32*, 119–135.

Hart, W. K., J. L. Aronson, and S. A. Mertzman (1984), Areal distribution and age of low-K, high-alumina olivine tholeiite magmatism in the northwestern Great Basin, *Geol. Soc. Am. Bull.*, *95*, 186–195.

Hill, B. E., and E. M. Taylor (1989), Oregon central high Cascades pyroclastic units in the vicinity of Bend, Oregon, *U.S. Geol. Surv. Open File Rep.*, *89–645*, 51–54.

Hooper, P. R. (1997), The Columbia River flood basalt province: Current status, in *Large Igneous Provinces, Continental, Oceanic, and Planetary Flood Volcanism*, *Geophys. Monogr. Ser.*, vol. 100, edited by J. J. Mahoney and M. F. Coffin, pp. 1–27, AGU, Washington, D. C.

Hooper, P. R., G. B. Binger, and K. R. Lees (2002), Ages of the Steens and Columbia river flood basalts and their relationship to extension-related calc-alkaline volcanism in eastern Oregon, *Geol. Soc. Am. Bull.*, *114*, 43–50.

Humphreys, E. D., K. G. Dueker, D. L. Schutt, and R. B. Smith (2000), Beneath Yellowstone: Evaluating plume and nonplume models using teleseismic images of the upper mantle, *GSA Today*, *10*, 1–7.

Ito, G., J. Lin, and D. Graham (2003), Observational and theoretical studies of the dynamics of mantle plume-mid-ocean ridge interaction, *Rev. Geophys.*, *41*(4), 1017, doi:10.1029/2002RG000117.

Johnson, J. A. (1998), Geologic map of the Frederick Butte volcanic center, Dechutes and Lake Counties, south-central Oregon, *U.S. Geol. Surv. Open File Rep.*, *98–208*.

Johnson, J. A., and A. L. Grunder (2000), The making of intermediate composition magma in a bimodal suite: Duck Butte Eruptive Center, Oregon, USA, *J. Volcanol. Geotherm. Res.*, *95*, 175–195.

Jordan, B. T. (2001), Reconciling the misfit between the Yellowstone plume trace and global plate motion models: Channelized and pancake plume flow on basal lithospheric topography, *Eos Trans. AGU*, *82*(47), Fall Meet. Suppl., Abstract T42C-0953.

Jordan, B. T. (2004), Age-progressive volcanism of the Oregon High Lava Plains: Overview and evaluation of tectonic models, in *Plumes, Plates, and Paradigms*, edited by G. R. Foulger et al., *Spec. Pap. Geol. Soc. Am.*, in press.

Jordan, B. T., D. W. Graham, and A. L. Grunder (2000), Do helium isotopes in basalts of the Oregon High Lava Plains implicate a Yellowstone plume component?, *Geol. Soc. Am. Abstr. Programs*, *32*(7), 150.

Jordan, B. T., M. J. Streck, and A. L. Grunder (2002a), Bimodal volcanism and tectonism of the High Lava Plains, Oregon, in *Field Guide to Geologic Processes in Cascadia*, edited by G. Moore, *Spec. Pap. Oreg. Dep. Geol. Miner. Ind.*, *36*, 23–46.

Jordan, B. T., A. L. Grunder, and B. K. Nelson (2002b), Basaltic volcanism of the Oregon High Lava Plains, *Geol. Soc. Am. Abstr. Programs*, *34*(5), 37.

Lawrence, R. D. (1976), Strike-slip faulting terminates the Basin and Range province in Oregon, *Geol. Soc. Am. Bull.*, *87*, 846–850.

Linneman, S. K., and J. D. Meyers (1990), Magmatic inclusions in Holocene rhyolites of Newberry volcano, central Oregon, *J. Geophys. Res.*, *95*, 17,677–17,699.

MacLean, J. W. (1994), Geology and Geochemistry of Juniper Ridge, Horsehead Mountain and Burns Butte: Implications for the petrogenesis of silicic magmas on the High Lava Plains, southeastern Oregon, M.S. thesis, 141 pp., Oreg. State Univ., Corvallis.

MacLeod, N. S., G. W. Walker, and E. H. McKee (1975), Geothermal significance of eastward increase in age of Upper Cenozoic rhyolitic domes in southeastern Oregon, *U.S. Geol. Surv. Open File Rep.*, *75–348*, 21 pp.

Magill, J., and A. Cox (1981), Post-Oligocene tectonic rotation of the Oregon Western Cascade Range and Klamath Mountains, *Geology*, *9*, 127–131.

Mahon, K. I. (1996), The new "York" regression: Application of improved statistical method to geochemistry, *Int. Geol. Rev.*, *38*, 293–303.

McKee, E. H., and G. W. Walker (1976), Potassium-argon ages of late Cenozoic silicic volcanic rocks, southeastern Oregon, *Isochron West*, *15*, 37–41.

Müller, R. D., J.-Y. Royer, and L. A. Lawver (1993), Revised plate motions relative to the hotspots from combined Atlantic and Indian Ocean hotspot tracks, *Geology*, *21*, 275–278.

Pickthorn, L. B. G., and D. R. Sherrod (1990), Potassium-argon ages from the Klamath Falls area, south-central Oregon, *Isochron West*, *55*, 13–17.

Pierce, K. L., and L. A. Morgan (1992), The track of the Yellowstone hotspot: Volcanism, faulting, and uplift, in *Regional Geology of Eastern Idaho and Western Wyoming*, edited by K. Link, M. A. Kuntz, and L. B. Platt, *Mem. Geol. Soc. Am.*, *179*, 1–53.

Pierce, K. L., L. A. Morgan, and R. W. Saltus (2000), Yellowstone plume head: Postulated relations to the Vancouver slab, continental boundaries, and climate, *U.S. Geol. Surv. Open File Rep., 00–498*, 39 pp.

Priest, G. R. (1990), Volcanic and tectonic evolution of the Cascade volcanic arc, central Oregon, *J. Geophys. Res.*, *95*, 19,583–19,599.

Renne, P. R., A. L. Deino, R. C. Walter, B. D. Turrin, C. C. Swisher, T. A. Becker, G. H. Curtis, W. D. Sharp, and A.-R. Jaouni (1994), Intercalibration of astronomical and radioisotopic time, *Geology*, *22*, 783–786.

Rodgers, D. W., M. Estes, C. Meehan, T. Osier, J. Preacher, and L. Warren (1994), Style, kinematics, and timing of Neogene–Quaternary extension in the northern Basin and Range, *Geol. Soc. Am. Abstr. Programs*, *34*(6), 61.

Rodgers, D. W., H. T. Ore, R. Bobo, N. McQuarrie, and N. Zentner (2004), Extension and subsidence of the eastern Snake River Plain, in *Tectonic and Magmatic Evolution of the Snake River Plain Volcanic Province*, *Idaho Geol. Surv. Bull. 30*, edited by B. Bonnichsen, M. O. McCurry, and C. White, pp. 121–155, Idaho Geol. Surv., Moscow, Idaho.

Sarna-Wojcicki, A. M., C. E. Meyers, J. K. Nahata, W. E. Scott, B. E. Hill, J. L. Slate, and P. C. Russell (1989), Age and correlation of mid-Quaternary ash beds and tuffs in the vicinity of Bend, Oregon, *U.S. Geol. Surv. Open File Rep.*, *89–645*, 55–62.

Sherrod, D. R., and J. G. Smith (2000), Geologic map of upper Eocene to Holocene volcanic and related rocks of the Cascade Range, Oregon, *U.S. Geol. Surv. Geol. Invest. Ser.*, *I-2560*.

Sleep, N. H. (1996), Lateral flow of hot plume material ponded at sublithospheric depths, *J. Geophys. Res.*, *101*, 28,065–28,083.

Smith, R. B., and L. W. Braille (1994), The Yellowstone hotspot, *J. Volcanol. Geotherm. Res.*, *61*, 121–188.

Steiger, R. H., and E. Jäger (1977), Subcommision on geochronology: Convention on the use of decay constants in geo- and cosmochronology, *Earth Planet. Sci. Lett.*, *36*, 359–362.

Steinberger, B. (2000), Plumes in a convecting mantle: Models and observations for individual hotspots, *J. Geophys. Res.*, *105*, 11,127–11,152.

Steinberger, B., and R. J. O'Connell (2000), Effects of mantle flow on hotspot motion, in *The History and Dynamics of Global Plate Motions*, *Geophys. Monogr. Ser.*, vol. 120, edited by M. A. Richards, R. G. Gordon, and R. D. van der Hilst, pp. 377–398, AGU, Washington, D. C.

Streck, M. J., and A. L. Grunder (1995), Crystallization and welding variations in a widespread ignimbrite sheet: The Rattlesnake Tuff, eastern Oregon, *Bull. Volcanol.*, *57*, 151–169.

Streck, M. J., and A. L. Grunder (1999), Enrichment of basalt and mixing of dacite in the rootzone of a large rhyolite chamber: Inclusions and pumices from the Rattlesnake Tuff, Oregon, *Contrib. Mineral. Petrol.*, *136*, 193–212.

Swanson, D. A. (1982), Volcanic Studies in the Pacific Northwest, 1879–1979, in *Frontiers of Geological Exploration of Western North America*, pp. 107–193, Pac. Div., Am. Assoc. for the Adv. of Sci., San Francisco, Calif.

Swisher, C. C., J. A. Ach, and W. K. Hart (1990), Laser fusion $^{40}Ar/^{39}Ar$ dating of the type locality Steens Basalt, southeast Oregon, and age of the Steens geomagnetic polarity transition, *Eos Trans. AGU*, *71*, 1296.

Takahahshi, E., N. Katshji, and T. L. Wright (1998), Origin of the Columbia River basalts: Melting model of a heterogeneous plume head, *Earth Planet. Sci. Lett.*, *162*, 63–80.

Thompson, R. N., and S. A. Gibson (1991), Subcontinental mantle plumes, hotspots, and pre-existing thinspots, *J. Geol. Soc. London*, *148*, 973–977.

Walker, G. W. (1969), Geology of the High Lava Plains province, in *Mineral and Water Resources of Oregon*, edited by A. E. Weissenborn, *Oreg. Dep. Geol. Mineral. Ind. Bull.*, *64*, 77–79.

Walker, G. W. (1974), Some implications of Late Cenozoic volcanism to geothermal potential in the High Lava Plains of south-central Oregon, *Ore Bin*, *36*, 109–119.

Walker, G. W., and N. S. MacLeod (1991), Geologic map of Oregon, U.S. Geol. Surv., Reston, Va.

Wells, R. E., and P. L. Heller (1988), The relative contribution of accretion, shear, and extension to tectonic rotation in the Pacific Northwest, *Geol. Soc. Am. Bull.*, *110*, 325–338.

A. L. Deino, Berkeley Geochronology Center, 2455 Ridge Road, Berkeley, CA 94709, USA. (adeino@bgc.org)

R. A. Duncan, College of Oceanic and Atmospheric Sciences, Oregon State University, Ocean Administration Bldg. 104, Corvallis, OR 97331-5503, USA. (rduncan@coas.oregonstate.edu)

A. L. Grunder, Department of Geosciences, Oregon State University, Wilkerson Hall 104, Corvallis, OR 97331-5506, USA. (grundera@bcc.orst.edu)

B. T. Jordan, Department of Geology, College of Wooster, 1189 Beall Avenue, Wooster, OH 44691, USA. (bjordan@wooster.edu)